TECHNICAL REPORT STANDARD TITLE PAGE

1. Report No.	2. Government Accession No.	3. Recipient's Catalog No.
FHWA/TX-86/48+386-2F		

4. Title and Subtitle	5. Report Date
EFFECT OF TRUCK TIRE INFLATION PRESSURE AND AXLE LOAD ON PAVEMENT PERFORMANCE	August 1985
	6. Performing Organization Code
7. Author(s)	8. Performing Organization Report No.
Kurt M. Marshek, W. Ronald Hudson, Hsien H. Chen, Chhote L. Saraf, and Richard B. Connell	Research Report 386-2F
9. Performing Organization Name and Address	10. Work Unit No.
Center for Transportation Research The University of Texas at Austin Austin, Texas 78712-1075	11. Contract or Grant No. Research Study 3-8-84-386
	13. Type of Report and Period Covered
12. Sponsoring Agency Name and Address Texas State Department of Highways and Public Transportation; Transportation Planning Division P. O. Box 5051 Austin, Texas 78763	Final
	14. Sponsoring Agency Code

15. Supplementary Notes

Study conducted in cooperation with the U. S. Department of Transportation, Federal Highway Administration. Research Study Title: "The Magnitude of Tire Pressures on Texas Highways and the Effect of Tire Pressures on Flexible and Rigid Pavements"

16. Abstract

This report presents the results of an investigation into the effect of truck tire inflation pressure and axle load on flexible and rigid pavement performance as determined using computer analysis.

The flexible pavement analysis was conducted with both a nonuniform pressure model and a uniform pressure model as input to the elastic layer program BISAR and the 3D finite element program TEXGAP-3D. The results show that (1) the uniform pressure model overestimated the increase in tensile strain at the bottom of the surface for overinflated tires, and underestimated the increase in tensile strain at the bottom of the surface for overloaded tires, (2) both high inflation pressure and heavy load caused a high increase in tensile strain at the bottom of the surface and a significant reduction of the pavement fatigue damage life, and (3) the axle load (not the inflation pressure) played a major role in the subgrade rutting life.

A rigid pavement analysis was conducted with both a nonuniform pressure model and a uniform pressure model as input to the program JSLAB. The difference between the results obtained for the nonuniform model and those for the uniform pressure model for the same axle load is insignificant.

17. Key Words	18. Distribution Statement
tire pressures, flexible pavements, rigid pavements, distress prediction, contact pressure distribution, pavement analysis	No restrictions. This document is available to the public through the National Technical Information Service, Springfield, Virginia 22161.

19. Security Classif. (of this report)	20. Security Classif. (of this page)	21. No. of Pages	22. Price
Unclassified	Unclassified	86	

Form DOT F 1700.7 (8-69)

EFFECT OF TRUCK TIRE INFLATION PRESSURE AND AXLE LOAD ON PAVEMENT PERFORMANCE

by

Kurt M. Marshek
W. Ronald Hudson
Hsien H. Chen
Chhote L. Saraf
Richard B. Connell

Research Report Number 386-2F

The Magnitude of Tire Pressures on Texas Highways
and the Effect of Tire Pressures on Flexible and Rigid Pavements
Research Project 3-8-84-386

conducted for

Texas State Department of Highways and
Public Transportation

in cooperation with the
U. S. Department of Transportation
Federal Highway Administration

by the

Center for Transportation Research
The University of Texas at Austin

August 1985

The contents of this report reflect the views of the authors, who are responsible for the facts and the accuracy of the data presented herein. The contents do not necessarily reflect the official views or policies of the Federal Highway Administration. This report does not constitute a standard, specification, or regulation.

There was no invention or discovery conceived or first actually reduced to practice in the course of or under this contract, including any art, method, process, machine, manufacturer, design or composition of matter, or any new and useful improvement there of, or any variety of plant which is or may be patentable under the patent laws of the United States of America or any foreign country.

PREFACE

This is the second of two reports which describe work done on Project 386, "The Magnitude of Tire Pressures on Texas Highways and the Effect of Tire Pressures on Flexible and Rigid Pavements." This study was conducted at the Center for Transportation Research (CTR), The University of Texas at Austin, as part of a cooperative research program sponsored by the Texas State Department of Highways and Public Transportation and the Federal Highway Administration.

Many people have contributed their help toward the completion of this report. Thanks are extended to Dr. B. F. McCullough for his help and guidance and to all the CTR personnel, especially Lyn Gabbert, Raul Longoria, Monica Gonzalez, Loretta McFadden, Art Frakes, John Ermis, Donna Williams, and Kitty Collins. Invaluable comments were provided by Robert L. Mikulin, Jerome F. Daleiden, and James L. Brown, all from the Texas State Department of Highways and Public Transportation and by Edward V. Kristaponis from the Federal Highway Administration.

Kurt M. Marshek
W. Ronald Hudson
Hsien H. Chen
Chhote L. Saraf
Richard B. Connell

LIST OF REPORTS

Report No. 386-1, "Experimental Investigation of Truck Tire Inflation Pressure on Pavement-Tire Contact Area and Pressure Distribution," by Kurt M. Marshek, W. Ronald Hudson, Richard B. Connell, Hsien H. Chen, and Chhote L. Saraf, presents data on the effect of truck tire pressure and load on contact area, and pressure distribution. August 1985.

Report No. 386-2F, "Effect of Truck Tire Inflation Pressure and Axle Load on Pavement Performance," by Kurt M. Marshek, W. Ronald Hudson, Hsien H. Chen, Chhote L. Saraf, and Richard B. Connell, presents an analytical evaluation of the effect of truck tire inflation pressure on pavement performance. August 1985.

ABSTRACT

This report presents the results of an investigation into the effect of truck tire inflation pressure and axle load on flexible and rigid pavement performance as determined using computer analysis.

The flexible pavement analysis was conducted with both a nonuniform pressure model and a uniform pressure model as input to the elastic layer program BISAR and the 3D finite element program TEXGAP-3D. The results show that (1) the uniform pressure model overestimated the increase in tensile strain at the bottom of the surface for overinflated tires, and underestimated the increase in tensile strain at the bottom of the surface for overloaded tires, (2) both high inflation pressure and heavy load caused a high increase in tensile strain at the bottom of the surface and a significant reduction of the pavement fatigue damage life, and (3) the axle load (not the inflation pressure) played a major role in the subgrade rutting life.

A rigid pavement analysis was conducted with both a nonuniform pressure model and a uniform pressure model as input to the program JSLAB. The difference between the results obtained for the nonuniform model and those for the uniform pressure model for the same axle load is insignificant.

Key words: tire pressures, flexible pavements, rigid pavements, distress prediction, contact pressure distribution, pavement analysis.

SUMMARY

The main contributions of this report are results showing the effects of tire contact pressures and axle loads on flexible pavement performance with particular attention to fatigue life and rutting using layer programs (BISAR, ELSYM5), and a finite element program TEXGAP-3D. The results can be summarized as follows: (1) both high inflation pressure and heavy axle load cause a high increase in tensile strain at the bottom of the surface layer and a significant reduction of the pavement fatigue damage life, (2) the axle load, instead of the inflation pressure, plays a major role in the subgrade rutting life, (3) the uniform pressure model (which is commonly used for pavement design) overestimates the increase in tensile strain at the bottom of the surface layer for overinflated tires, and underestimates the increase in tensile strain at the bottom of the surface layer for overloaded tires, (4) tread type (bald or treaded tire) has a small effect on the critical tensile strains developed in the surface course, (5) the addition of tangential loading (braking force) to normal loading produces a higher strain than the pure normal loading condition, and (6) the effect of contact pressure distribution (for the same axle load) on rigid pavement tensile stress at the bottom of the surface layer is not significant.

IMPLEMENTATION STATEMENT

The work carried out under this project provides highway design engineers with information useful for evaluating the effect of tire inflation pressure on the structural adequacy and capacity of flexible and rigid pavements. Such information hopefully will lead to changes in the methods employed for current highway design and thereby lead to improvements in the structural capacity of pavements and/or overlay design or produce recommendations for legislation to regulate truck tire inflation pressure or axle load.

TABLE OF CONTENTS

CHAPTER 1. INTRODUCTION

Truck tire pressures in Texas have increased in the last few years. The increased surface rutting in asphaltic concrete pavements and decreased fatigue life in asphaltic concrete and Portland cement concrete pavements are suspected as being related to higher truck tire pressures. No truly basic research has been done on determining the effect of tire inflation pressure on pavement loading in recent years.

A previous report (Ref. 1), entitled "Experimental Investigation of Truck Tire Inflation Pressure on Pavement-Tire Contact Area and Pressure Distribution," presents results showing experimental contact pressure distributions for truck tires loaded at different axle loads and at various tire inflation pressures.

This report deals with the effect of tire pressures on flexible and rigid pavement performance. Special emphasis is placed on investigating the effects of tire pressure change on flexible and rigid pavement performance. This investigation was intended to quantify the effects of increasing tire pressure. A detailed description of the analysis and the results is presented.

BACKGROUND

A variety of factors are known to contribute to pavement damage, including climate, traffic density, and the loads from car and truck tires. Historically, the subject of the effect of truck tire inflation pressure has received little attention for several reasons: simplifying assumptions made in past pavement design procedures have made knowledge of the actual tire-pavement contact pressure distribution unnecessary, and measurements of the contact pressure over the entire contact area are difficult. The influence of tire inflation pressure and the contact pressure distribution between the tire and the pavement will both undoubtedly play a larger role in pavement design once their role in causing pavement damage is better understood.

Love and Burmister (Refs 2 and 3) first modeled the tire load as a circular uniform pressure distribution; only the inflation pressure and axle load were considered important. The uniform pressure tire model continued to be commonly used in highway design. Duncan, Monismith, and Wilson (Ref 4) used a uniform pressure distribution model and a finite element technique to analyze the stress conditions that occur below the tire-pavement interface. They studied a pavement three-dimensionally using a two-dimensional axisymmetric layer model.

OBJECTIVES

The main objective of this report is to determine the effect of tire inflation pressure, tire axle load, tire tread type, and friction (braking force) on the stresses and strains in flexible and rigid pavements. Emphasis is placed on investigating the effects of high inflation pressure and heavy load on the tensile strain at the bottom of the surface (which is associated with fatigue cracking) and the compressive strain at the top of the subgrade (which is associated with subgrade rutting) by using both a nonuniform circular pressure model (BISAR) and a 3D finite element model (TEXGAP-3D). A portion of the study will investigate the effect of pressure distributions on the critical tensile stresses at the bottom of a rigid pavement surface layer.

SCOPE AND ORGANIZATION

Chapter 1 provides an introduction to this report.

Chapter 2 presents the results showing the effect of inflation pressure, tread type, tangential friction, and axle load on the asphalt concrete pavement critical surface tensile strain and critical subgrade compressive strain using the nonuniform circular pressure model (BISAR).

In Chapter 3, the 3D finite element model (TEXGAP-3D) is used to investigate the effect of high inflation pressure and heavy axle load on (1) the critical tensile strain at the bottom of the asphalt concrete surface, (2) the compressive strain at the top of the subgrade, and (3) the pavement damage life.

Chapter 4 presents results for the rigid pavement stress analysis. Conclusions and recommendations made throughout the report are summarized in Chapter 5.

CHAPTER 2. FLEXIBLE PAVEMENT ANALYSIS -- AN AXISYMMETRIC LAYER MODEL

A previous report (Ref. 1) presents results showing experimental nonuniform contact pressure distributions for truck tires loaded at different axle loads and at various tire inflation pressures. This experimental data was obtained in order to determine what effect the magnitude and shape of the pressure distribution has on the stresses, strains, and deformations developed in the pavement as a result of truck tire loading. Computer programs typical of those used by highway engineers in pavement analysis and design work are used to determine the strains and stresses of interest for both flexible and rigid pavements. The strains and stresses for a treaded tire contact pressure distribution are compared to those obtained using the traditional design assumptions.

The objective of this chapter is to determine the effect of tire inflation pressure, tire axle load, and tire pressure distribution on the strains and stresses in flexible pavement. A large portion of this chapter concentrates on flexible pavements owing to their anticipated sensitivity to the pressure distribution. The pavement descriptions and computer models used in the analysis of pavement performance are also described.

FLEXIBLE PAVEMENT MODEL

Figure 2.I shows the flexible pavement model with surface, base, and subgrade courses. The surface courses in this study had thicknesses (H_S) of between one and four inches and a modulus of elasticity (E) of 400 ksi. The base and subgrade had thicknesses of 8 inches and 169 inches, respectively, and Young's moduli of 20 ksi and 6 ksi. The course thicknesses and moduli of elasticity chosen correspond with those of a low volume road.

FLEXIBLE PAVEMENT ANALYSIS PROGRAM (BISAR)

There are a number of computer programs available that can be used to analyze pavement performance. The choice of a particular program depends on a number of parameters, including the following: the form of input, the characteristics of the simulated pavement, and the output variables desired from the analysis. Computer program BISAR (Ref 5) is used in this study to predict the performance of flexible pavements.

Computer program BISAR (BItumen Structures Analysis in Roads) has been devised as a general-purpose program for computing stresses, strains, and displacements in elastic multilayered systems subjected to one or more uniform loads, acting uniformly over circular surface areas. These surface loads can be combinations of a vertical normal pressure and a unidirectional tangential stress.

PRESSURE DISTRIBUTION MODEL FOR BISAR

BISAR uses a common form of data input, that of a uniform pressure acting on a circular area (see Fig 2.2) or that of concentric circles with different pressures acting on each annular area (see Fig 2.3).

The traditional approach assumes that the contact area is circular in shape, and that the contact pressure is uniform over the circular area and equal in magnitude to the tire inflation pressure (Ref 6). These assumptions simplify the equations used in the analysis.

A more realistic model of the pressure distribution is represented by Fig 2.3. A half-section view of this pressure distribution model (tread tire, inflation pressure of 75 psi, and axle load 4500 lbs)

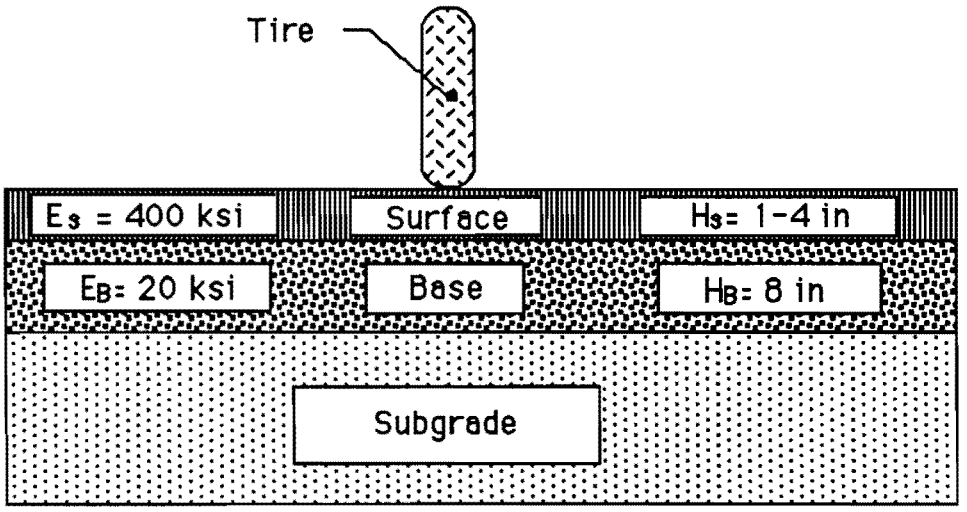

Fig 2.1. Diagram of a flexible pavement

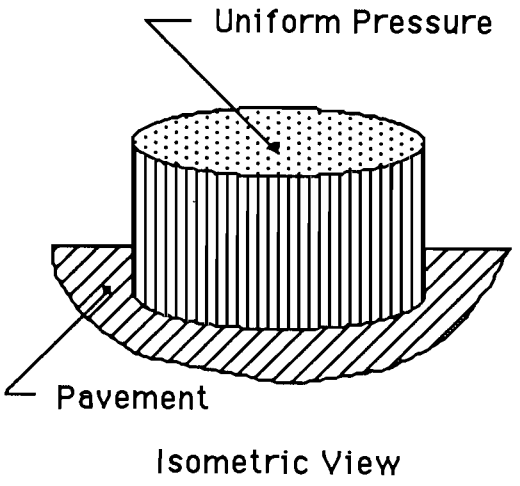

Fig 2.2. Uniform pressure distribution

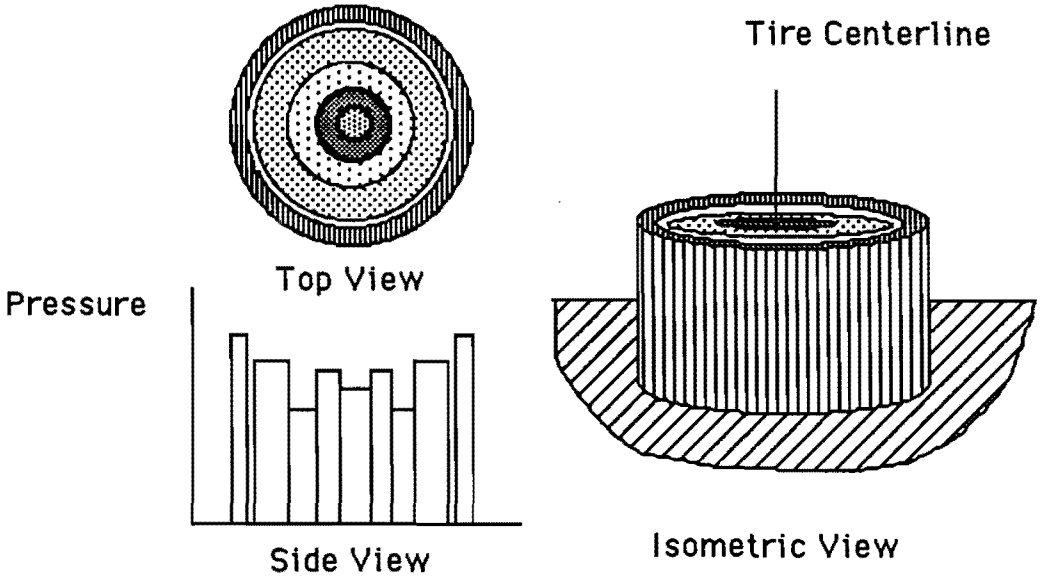

Fig 2.3. Concentric cylinder pressure distribution

which is used as input to program BISAR is shown in Fig 2.4. The computer input data is specified by a pressure distribution and the radial distances associated with each pressure level.

To match a given tire load, the radial distances are uniformly adjusted so that the sum of the forces (pressure intensity multiplied by the annular area on which it acts) equals the applied load. The form of data input, that of concentric circles, permits the use of pressure distributions containing localized annular regions of high pressure and the resulting large pressure gradients (such as those that occur at a tread gap and a tire shoulder). The pressure distribution inputs to BISAR for various tire inflation presures and axle loads studied in this chapter are given in Appendix A.

The contact pressure distribution was obtained experimentally using pressure sensitive film (Ref 1). Regions of interest (high contact pressure or large pressure gradients) along the tire contact width were visually identified from numerical prints of the experimental pressure distributions and then lines were drawn along the length of the print to identify these regions. The region of high contact pressure between the tire shoulder and circumferential gap was of special interest for this case due to the magnitude of the pressures that exist in the region. Therefore, this region was divided into four smaller areas to preserve the extremely high pressures (which occurred on a local level throughout this region) that would be lost if an averaging scheme were used over a larger area. Relatively low pressures from the gap to the tire centerline make this region less significant in the analysis; therefore, larger areas were used in this region. The distance between the tire centerline and the section line is an approximate radial distance.

A representative pressure distribution is obtained by drawing two lines across the tire print. This creates 14 enclosed regions containing different pressure values in each region. Averaging the pressures in each region then determines the pressure that acts on the corresponding annular area of the input pressure profile.

The radial distances defining the areas on which the pressures act were adjusted so that the total tire load equaled that used in obtaining the experimental data. This step was necessary since the experimental and input pressure distributions have different forms. For example, the high pressures that act only at the tire shoulder in the experimental distribution completely encircle the print on the computer input model. The radial distances are adjusted in a manner that keeps the relative size of each region proportional to the corresponding region on the actual tire footprint.

COMPUTER MODEL BISAR

The flexible pavement modeled with program BISAR consists of three courses (surface, base, and subgrade) with full friction between adjoining layers. The thickness of the course, modulus of elasticity, and Poisson's ratio for each course are assumed uniform throughout the pavement and are specified as input to BISAR. The frictional condition (no friction or no slip) that exists between adjacent courses is also user specified (Ref 5).

The output variables of BISAR are the stresses, strains, and deflections developed in each course in response to the applied load. Strain is the most useful variable when dealing with flexible pavements since theoretical relationships used in pavement design generally involve the strains developed in each course. The tensile strain at the bottom of the surface course and the compressive strain at the top of the subgrade were studied since they are known to contribute to pavement damage.

Damage to flexible pavements is caused by a number of different mechanisms, with the resulting damage usually being indicative of the mechanism involved. Since the computer analyses were conducted with the intent of showing the effect of the pressure distribution model on pavement performance, damage due to other mechanisms (such as frost heave, bleeding, pumping, and so on) was not considered. This leaves two major mechanisms to be addressed, the lateral movement of pavement material in the surface course and the vertical compaction of material in the three courses

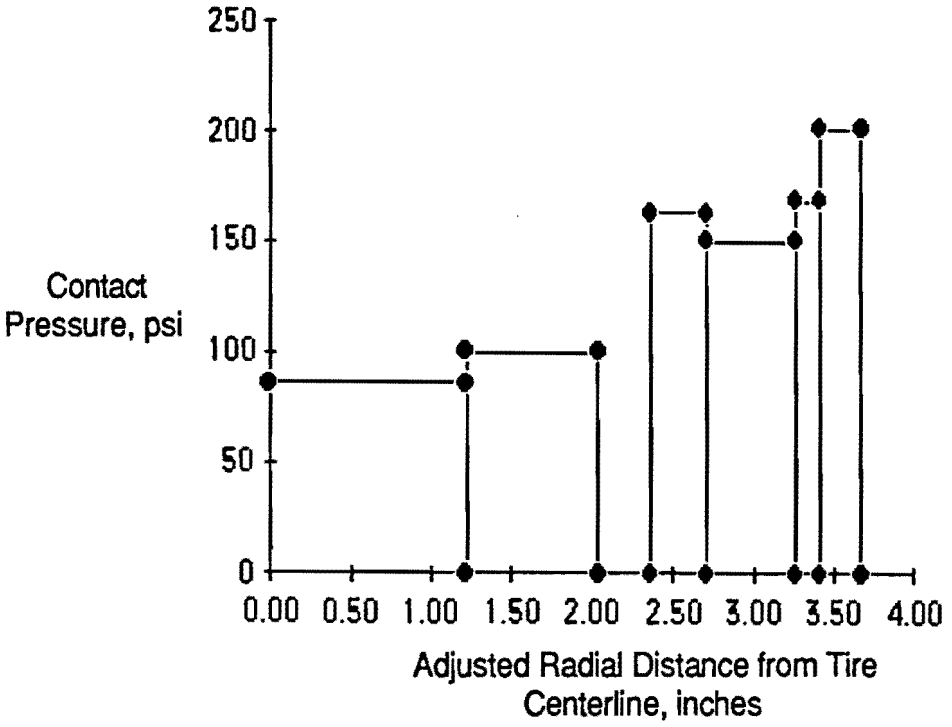

Fig 2.4. Sample input to computer program BISAR

(Ref 7).

When a surface course with a relatively high stiffness is subjected to high pressures or heavy loads, it is able to carry and transmit the loads without developing large compressive strains. However, the high stiffness causes large tensile and shear strains to be developed at the bottom of the surface course. The tensile and shear strains cause lateral movement of the material in the surface course away from the region below the tire contact zone and are responsible for longitudinal cracking. Due to the fact that an increase in tensile strain is always accompanied by an increase in horizontal shear strain, the effects of the pressure distribution on only the tensile strain was considered since similiar trends can be expected with the shear strain (Ref 7).

Compressive strains are more of interest when a surface course with low surface stiffness is used. In this case, high compressive strains are found in all the pavement layers in response to a heavy tire load. These strains, particularly those in the subgrade, are reponsible for most of the observed rutting. Past studies have shown that 70 to 95 percent of the compressive strain is found in the subgrade layer; therefore, the vertical compressive strain at the top of the subgrade is of most interest (Ref 7). This strain will be the second output variable (the tensile strain at the bottom of the surface course being the first) of interest from computer program BISAR.

PRESENTATION AND DISCUSSION OF RESULTS

Computer program BISAR was used in the flexible pavement analysis to determine the strains and stresses that occur throughout a pavement structure in response to various truck tire loadings. Results are presented showing the effect of tangential braking force, tread type, inflation pressure, and axle load on the stresses and strains developed in flexible pavements.

Effect of Tangential Braking Force on Tensile Strain at the Bottom of the Surface Course

Figure 2.5 shows the tensile strain at the bottom of the surface course for the case of the treaded tire at 90 psi inflation pressure and an axle load of 4500 lbf. The plot shows the pure normal loading case as well as the case where a tangential load (i.e., one developed during braking) equal to 30 % of the normal is superimposed onto the normal load. The strain for both cases is the same under the center of the tire. However, the tangential load produces higher strains elsewhere, with a maximum difference of about 13% being observed at a radial distance of 2.5 inches.

Effect of Tread Type on Tensile Strain at the Bottom of the Surface Course

Figure 2.6 shows the effect of the tread type on critical tensile strains at the bottom of a one-inch surface course for the treaded and bald tires at two different inflation pressures. Using a one-inch surface thickness permitted trends in strain to be more easily seen. A more realistic surface course would be 2 to 4 inches thick when normal-to-heavy wheel loads were anticipated (Ref 8).

At the same axle load, the treaded tire generally produces higher tensile strains than the bald, except for the underinflated case. When underinflated, the bald tire maintains a higher average pressure under the center of the tire (less shoulder effect) causing the strains to be higher at radial distances of roughly 1.5 inches and less. The treaded tire produces the tensile strain of greatest magnitude because of the regions of high pressure near the tire shoulder.

The critical tensile strains produced by three different pressure input models (i.e., bald, treaded, uniform) are shown plotted against surface course thickness in Figs 2.7 and 2.8. For the underinflated case (Fig 2.7), the treaded tire distribution produces much higher strains for thin surface thicknesses than does the bald tire distribution or uniform pressure model. As the surface thickness is increased, agreement between the three models improves; the models predict similiar results with

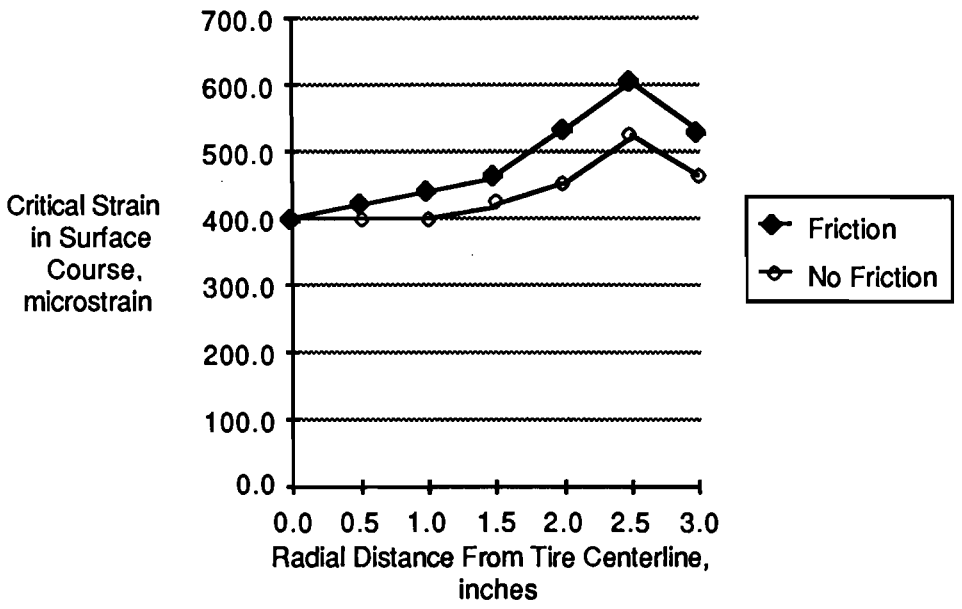

Fig 2.5 Effect of friction on tensile strain contour at the bottom of a one-inch-thick surface pavement

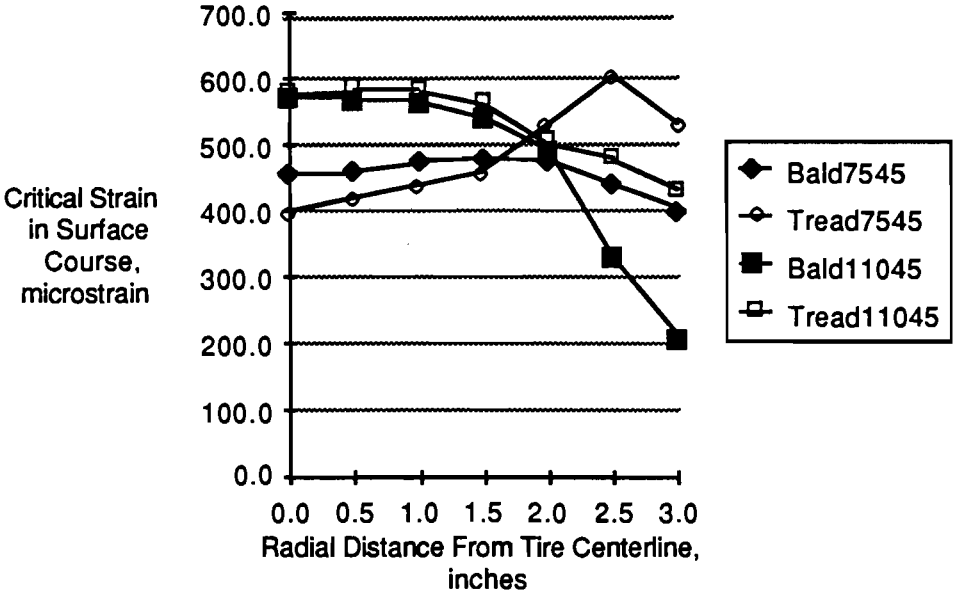

Note: Tread 7545 indicates the treaded tire at 75psi inflation pressure and axle load of 4500 lbf.

Fig 2.6 Effect of tread type on tensile strain contour at the bottom of a one-inch-thick surface pavement

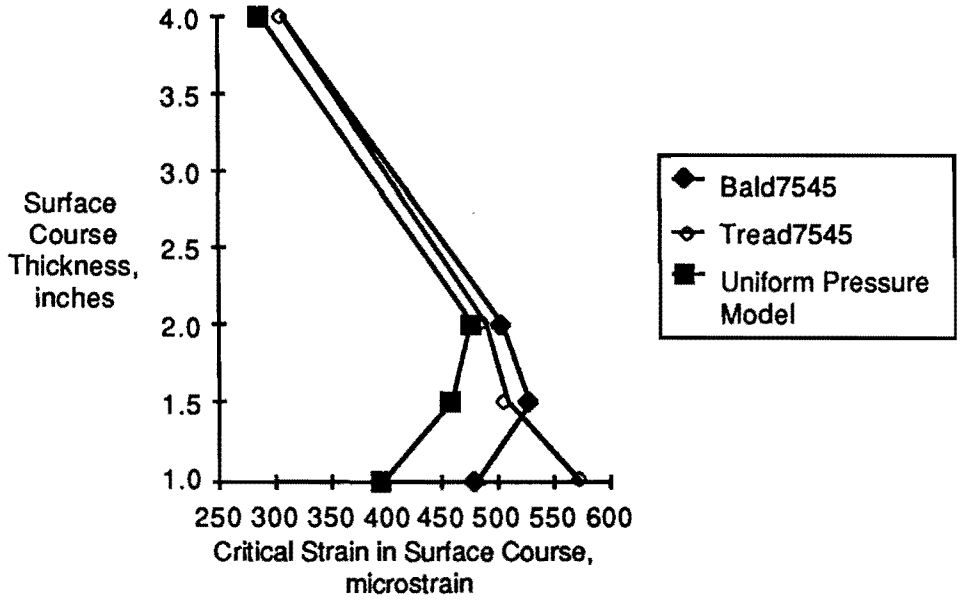

Fig 2.7 Effect of pressure distribution model on critical tensile strain at the bottom of the surface

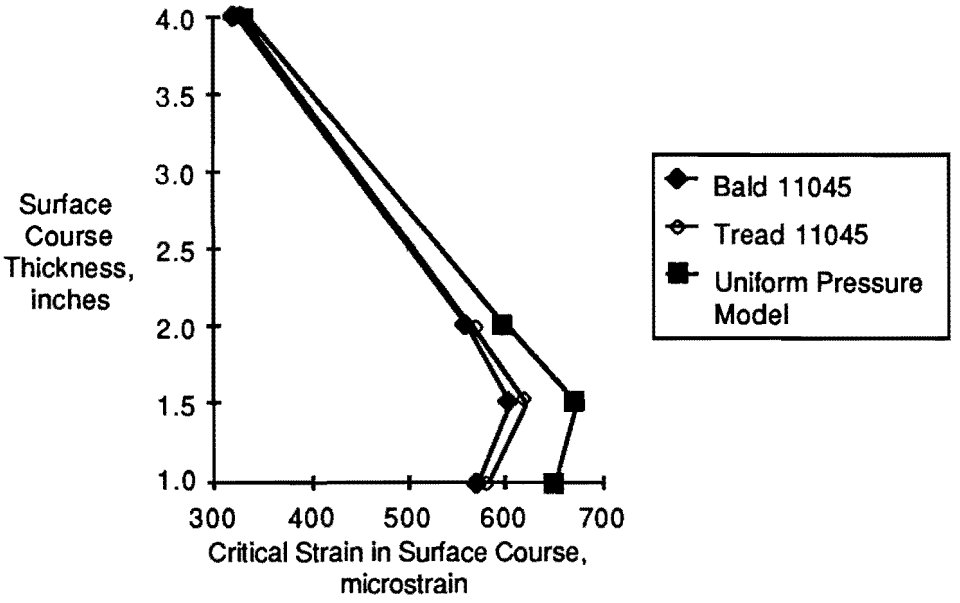

Fig 2.8 Effect of pressure distribution model on critical tensile strain at the bottom of the surface

surface thicknesses greater than about 2.5 inches. The uniform pressure model consistently underestimates the strains for the underinflated case.

Figure 2.8 shows that, for the overinflated case, the uniform pressure model always overestimates the strain produced. As before, the treaded tire produces larger strains than the bald tire for all surface thicknesses. In addition, the greatest difference between the strains produced for the three pressure distribution models occurs for thin surface layers.

Effect of Tire Inflation Pressure and Axle Load on Surface Tensile Strain

Figure 2.9 shows plots of the tensile strain at the bottom of the surface course for the treaded tire at three inflation pressures with a surface course thickness of one inch. This plot shows how inflation pressure determines the shape of the strain contour as well as the location of the maximum strain. For an underinflated tire, the high shoulder pressures produce the largest strains. Increasing the inflation pressure moves the highest strains towards the region beneath the center of the tire in response to the increased contact pressure on the corresponding area of the surface course.

Figure 2.10 shows the effect of inflation pressure on the critical tensile strains for surface course thicknesses from 1 to 4 inches. The overinflated tire consistently produces higher strains than the underinflated tire. For a typical surface course thickness (2 to 4 inches), the difference between the strains for the underinflated and overinflated cases is small.

Figure 2.11 shows the critical tensile strain developed at the bottom of the surface course by applying a 4500 lbf load and a 5400 lbf load to the threaded tire (at 90 psi rated inflation pressure). The maximum critical strain for the overloaded case occurs roughly 2.5 inches from the tire centerline; this is the expected result since it has been shown for the overloaded tire (Ref 1) that the region between the circumferential tread gap and the tire shoulder was saturated with high pressures (160 to 220 psi). For an increase in axle load of 20%, there is a corresponding 20% increase in the maximum critical tensile strain developed at the bottom of the surface course. Figure 2.12 shows the maximum critical strain obtained for two axle loads and the usual range of surface course thicknesses. As anticipated, the overloaded tire consistently produces the highest strains with a difference of about 20% being observed for a typical surface course thickness.

Effect of Tire Inflation Pressure and Axle Load on Subgrade Compressive Strain

In addition to the tensile strain in the surface course, the vertical compressive strain at the top of the subgrade (and how it is affected by the tire inflation pressure) is also of interest since this strain is known to play a major role in pavement damage. Figure 2.13 shows that an increase in inflation pressure produces a small increase in the compressive strain developed at the top of the subgrade for the usual range of surface course thicknesses.

The axle load has a significant effect on the compressive strains developed at the top of the subgrade. However, the axle load is unique (as compared with the other variables studied) in that its effect persists for all surface course thicknesses, as can be seen from Fig 2.14. The plot shows that a 20% increase in the axle load produces a 20% increase in the critical subgrade compressive strain for a typical surface course thickness.

SUMMARY

Based on the limited number of tire contact pressure distributions and pavements studied in this chapter, the following conclusions can be drawn:

(1) Superimposing a tangential load (braking force) onto the normal load has little effect on the

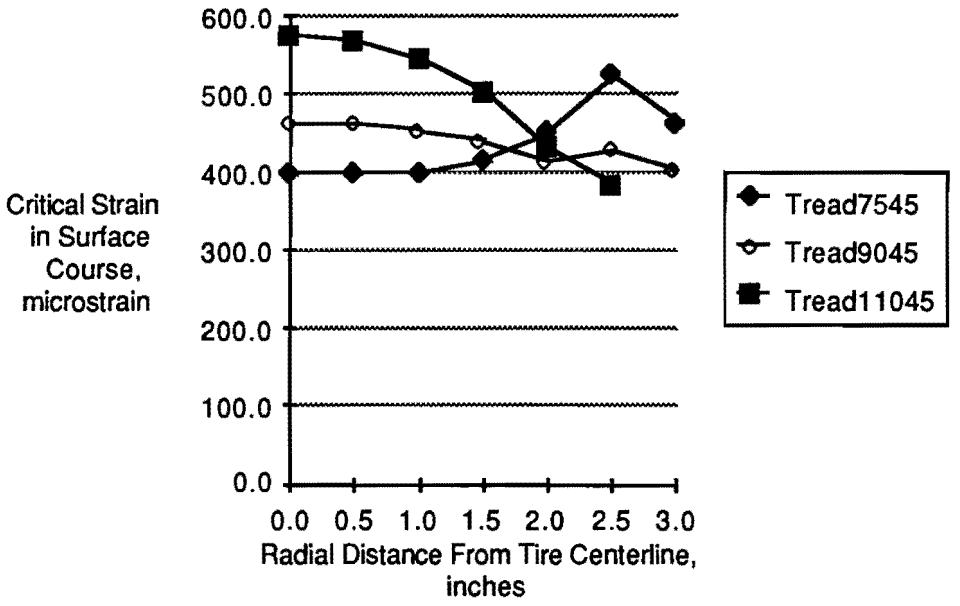

Fig 2.9 Effect of inflation pressure on tensile strains contour at the bottom of a one-inch-thick surface pavement

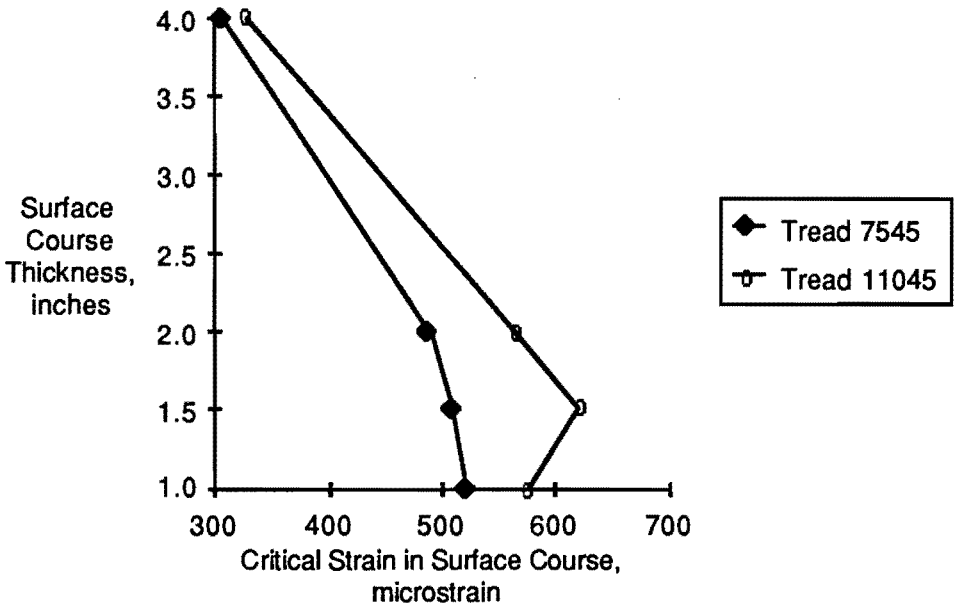

Fig 2.10 Effect of inflation pressure on critical tensile strains at the bottom of the surface

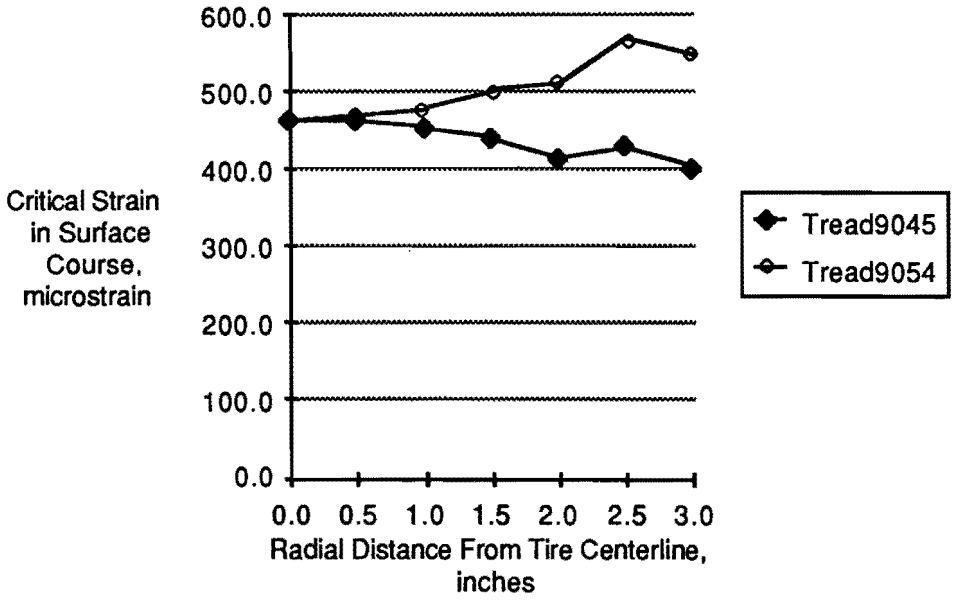

Fig 2.11 Effect of axle load on tensile strain contour at the bottom of a one-inch-thick surface pavement

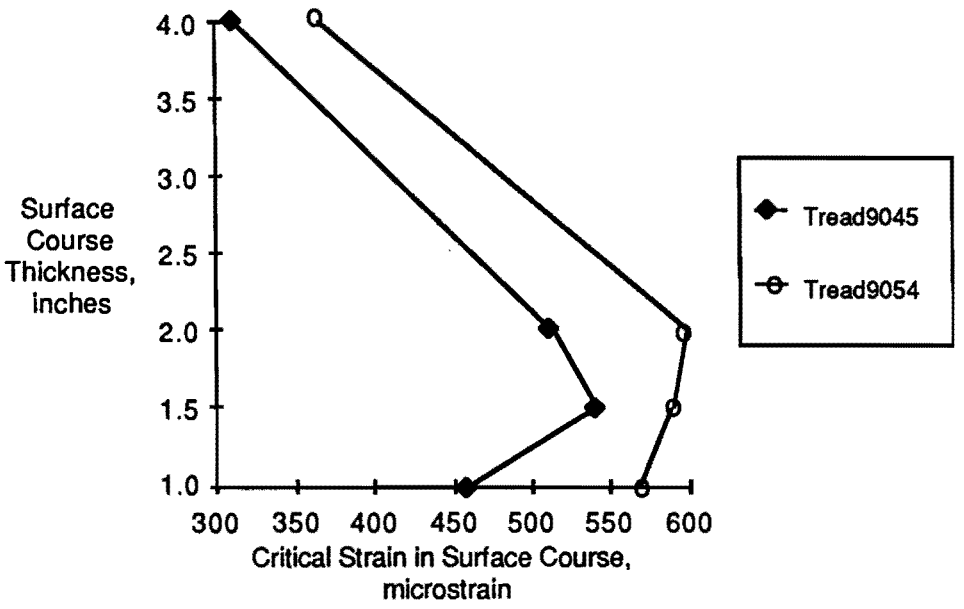

Fig 2.12 Effect of axle load on critical tensile strain at the bottom of the surface

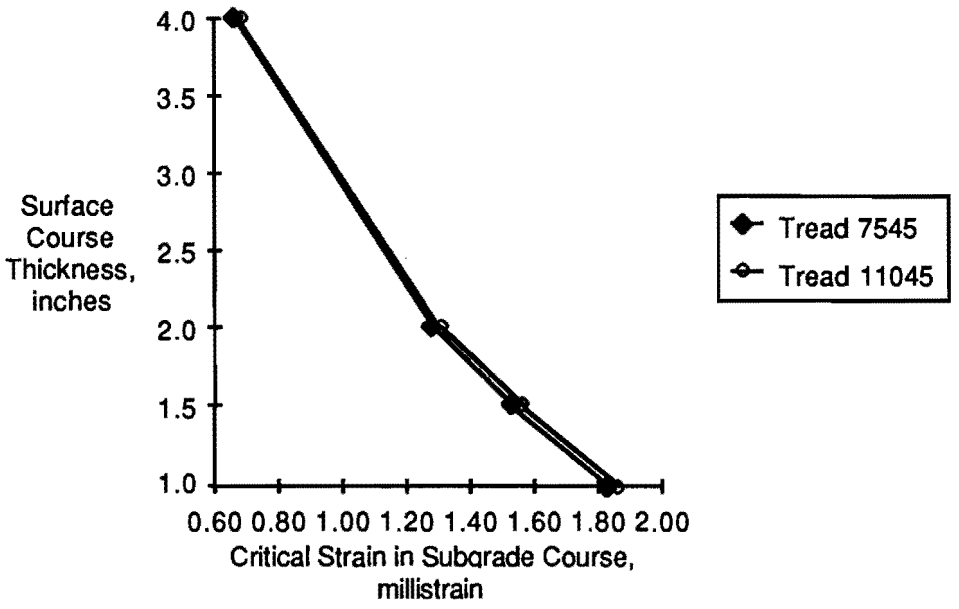

Fig 2.13 Effect of inflation pressure on critical compressive strain at the top of the subgrade

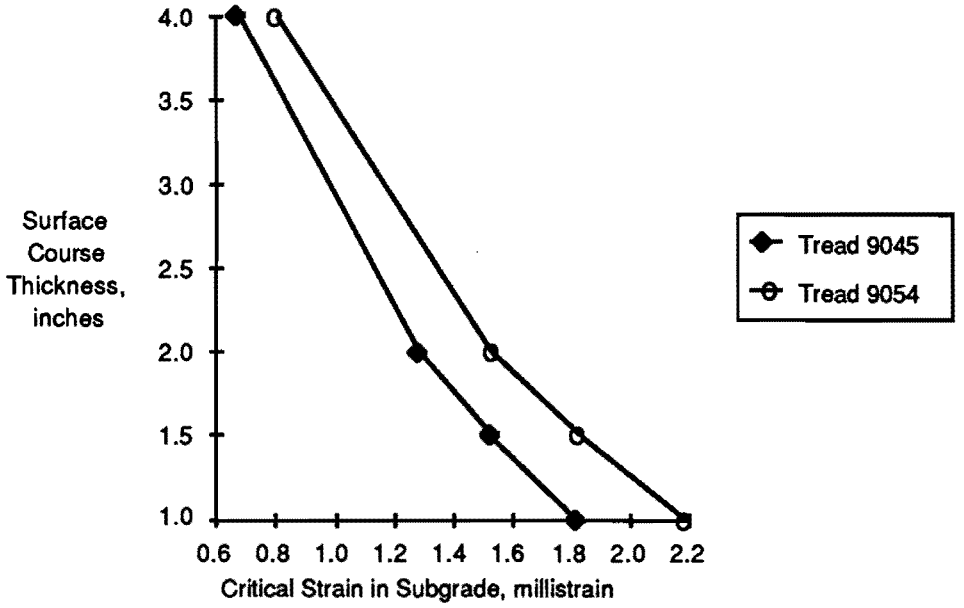

Fig 2.14 Effect of axle load on critical compressive strain at the top of the subgrade

tensile strains produced at the bottom of the surface course and under the center of the tire. With radial distances larger than about 1 inch, the effect of tangential braking force becomes more significant; the maximum difference in the surface tensile strains occurs at a radial distance of about 2.5 inches. The effect of tangential braking force, therefore, should be considered since it affects most strongly the strains of interest (the maximum tensile strains in the thin and flexible pavement).

(2) The tread type (bald or treaded tire) has a small effect on the critical tensile strains developed at the bottom of the surface course. A treaded tire produced slightly higher strains than the bald tire indicating that as a tire wears, there will be a small decrease in the maximum tensile strain produced.

(3) The tire inflation pressure has a greater effect than the tread type on the critical tensile strains at the bottom of the surface course. Inflation pressure determines not only the magnitude of the tensile strains produced, but also the location of the maximum tensile strain relative to the tire centerline. Underinflation produces a maximum strain under the tire shoulder; overinflation produces a maximum strain beneath the center of the tire. Although there is little difference in the magnitudes of the tensile strains produced for the two cases, especially when a realistic surface course thickness of 4 inches is used, the pavement life reduction due to high inflation pressure may be significant since strain ratio not the difference in strain is a significant factor in determining pavement damage life.

(4) The tire inflation pressure will have an effect of less than 2% effect on the compressive strains developed at the top of the subgrade. For surface course thicknesses between 2 and 4 inches, the effect of inflation pressure is negligible. Therefore, inflation pressure is an insignificant factor with respect to subgrade rutting.

(5) The axle load was the most significant factor causing high tensile strains at the bottom of the surface course in flexible pavements. Regions of high contact pressure (e.g., between the tire shoulder and circumferential gap) produce significant increases in the tensile strain with the maximum strains occuring below the high contact pressure regions. The increase in tensile strain at the bottom of the surface course is a function of the surface course thickness; the effect is most dramatic in pavements with thin surface courses. The axle load increases the tensile and horizontal shear strains in the surface course, making axle load the primary factor (among those studied) in causing fatigue cracking.

(6) The effect of the axle load on the critical compressive strains at the top of the subgrade persists for all surface course thicknesses. Increasing the axle load increases the maximum compressive strain by a proportional amount, regardless of surface course thickness. Therefore, axle load plays the dominant role in pavement damage with respect to surface and subgrade rutting.

CHAPTER 3. FLEXIBLE PAVEMENT ANALYSIS - A 3D FINITE ELEMENT MODEL

The previous chapter presented results showing the effect of high inflation pressures and heavy loads on the critical tensile strain at the bottom of the surface course and the compressive strain at the top of the subgrade by employing a nonuniform concentric circular pressure model. However, experimental results showed that the shoulder regions of a truck tire produce two strips of high pressure which can dominate the whole contact pressure distribution (Ref 1). Compared to the experimental tire contact pressure distribution, neither the uniform pressure model nor the nonuniform concentric circular pressure model appears appropriate as an input for pavement stress analysis.

The main objective of this chapter is to investigate the effects of high inflation pressures and heavy loads on the asphalt concrete pavement stress and pavement damage life by utilizing a 3D finite element model instead of the nonuniform circular pressure model. There are several general purpose finite element computer programs available that can be used to analyze pavement performance. For the three dimensional contact pressure model, computer program TEXGAP-3D was selected in this study to predict the performance of flexible pavements for various inflation pressures and truck tire axle loads. The disadvantage of accurately modeling the contact pressure distribution with a finite element analysis is the increased computation time. For example, the computation time for a single run on TEXGAP-3D (216 brick elements) was approximately 18 minutes, corresponding to $80 per case, as compared to 2.5 seconds execution time using the layer program ELSYM5.

FLEXIBLE PAVEMENT MODEL

The pavement selected for analysis is typical of that used on Texas farm to market roads. The modulus of elasticity, Poisson's ratio, and thickness of each layer are as follows:

Surface:		
	Thickness	1.5, 2.0, 3.0, and 4.0 inches
	Surface modulus	400 ksi
	Poisson's ratio	0.35
Base:		
	Thickness	8 inches
	Base modulus	60 ksi
	Poisson's ratio	0.40
Subgrade:		
	Thickness	169 inches
	Subgrade modulus	6 ksi
	Poisson's ratio	0.45

DESCRIPTION OF PROGRAM TEXGAP-3D

The finite element program TEXGAP-3D (Texas Grain Analysis Program) is a linear elastic, static finite element code for the analysis of a three dimensional continuum structure and as such is not a general purpose code because it does not contain other element types; i.e., beam, plate, and shell

elements. The element library includes quadratic, isoparametic 20 node bricks, 15 node triangular prisms, and 10 node tetrahedrons. Material models include isotropic, orthotropic, and anisotropic. Permissible loadings and boundary conditions include pressure and traction on a surface, sliding and clamped surfaces, and prescribed nodal point forces or displacements.

PRESSURE DISTRIBUTION MODEL FOR TEXGAP-3D

The total number of 3D solid brick elements and the corresponding computation time are plotted in Fig 3.1. Since the contact pressure distributions are quite symmetric along the tire center line, only one quarter of the tire pavement interaction was analysed, in order to minimize computer costs. The 3D finite element model (9x6x4) consists of 216 solid brick elements. The element size was smallest within the contact pressure region, as shown in the left hand corner of Fig 3.2. The pressure loading consists of 6x3 elements. Each element corresponds to an individual uniform contact pressure within the corresponding cell region. The pressure distributions (input to TEXGAP-3D for various inflation pressures and axle loads) studied in this chapter are given in Appendix B. The bottom of the subgrade was assumed rigid.

PAVEMENT DAMAGE

The two primary pavement distress conditions addressed in this analysis are fatigue and rutting. Fatigue cracks may develop if the tensile strain at the bottom of the asphalt layer is excessive. Rutting, the permanent deformation leading to loss of surface shape, may occur if the compressive strain at the top of the subgrade is excessive.

Fatigue Cracking Damage

Flexible pavement fatigue is manifest by the appearance of alligator cracking in the wheelpaths and is caused by excessive tensile stresses and strains at the bottom of the asphalt concrete surface layer. The tensile strains that have been computed using TEXGAP-3D at the bottom of the asphalt concrete surface are used to approximate the number of 18-kip axle load applications until Class 2 cracking occurs. Class 2 cracking is defined as the appearance of alligator cracking. Class 3 cracking is defined as the progression of alligator cracking to that of severe spalling. A pavement surface that has Class 2 cracking is assumed to have failed in fatigue.

Predictions of the number of loads (N_f) necessary to cause fatigue failure have been developed in the literature. Such predictions were based on laboratory tests, with little correlation to field experience to account for the relaxation times between traffic loads and the resulting differences in crack propagation rates. A literature survey showed that the number of wheel loads required to initiate fatigue distress is on the order of 13 to 18 times that predicted by constant-stress laboratory tests (Ref 9).

A field fatigue distress model can be developed for two levels of cracking: (1) cracking less than or equal to 10% of the wheelpath area; and (2) cracking equal to or greater than 45% of the wheelpath area. The equations presented are as follows (Ref 9):

$$\log N_f(\leq 10\%) = 15.947 - 3.291 \log \varepsilon_t - 0.854 \log E^* \quad (3.1)$$

$$\log N_f(\geq 45\%) = 16.086 - 3.291 \log \varepsilon_t - 0.854 \log E^* \quad (3.2)$$

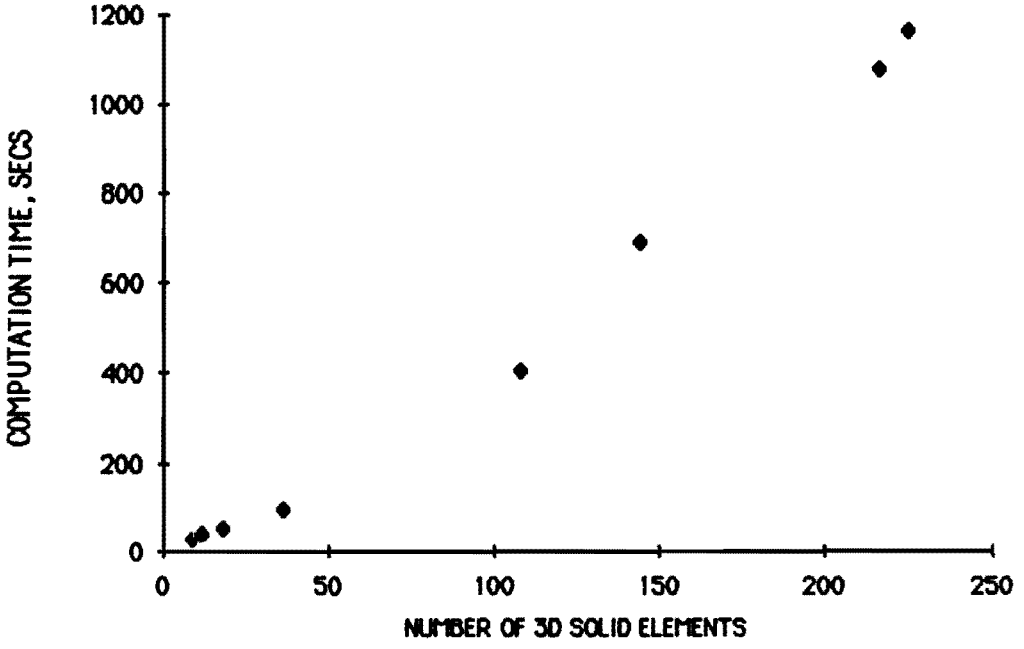

3.1 Number of 3D brick elements versus computation time

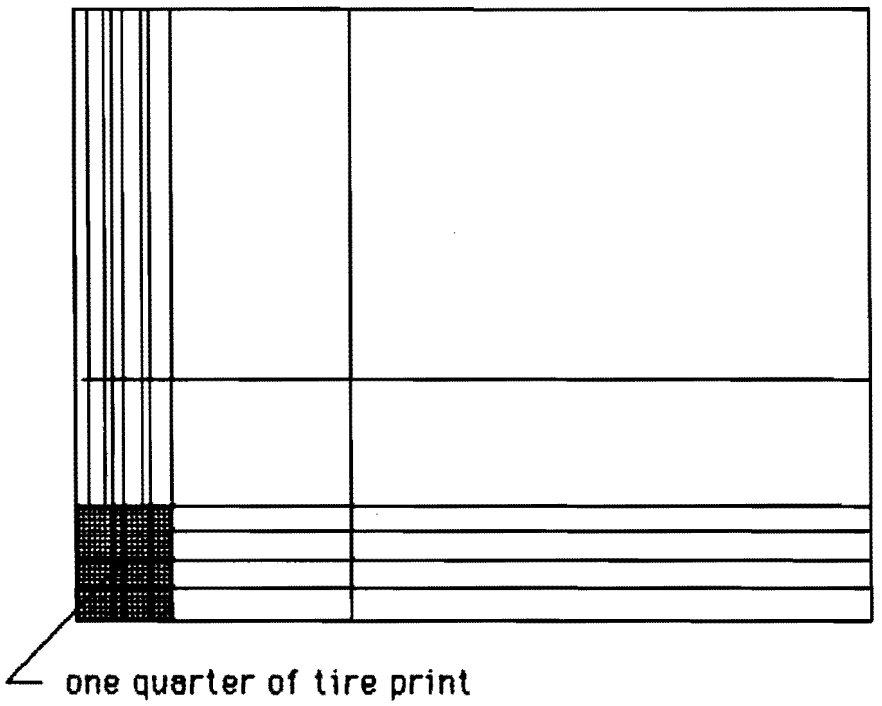

Fig. 3.2 Grid formulation at the surface of the asphalt concrete pavement (5 feet long by 5 feet wide)

where N_f = number of loads of constant stress necessary to cause fatigue cracking,

ϵ_t = initial tensile microstrain at the bottom of the surface, and

E^* = complex modulus of the asphalt concrete surface, ksi.

Rutting

Rutting in the wheelpaths results from high compressive strains and permanent deformation in one or more pavement layers. The amount of pavement rutting is determined by truck tire axle load, layer properties, environment, and number of traffic loadings. Analysis of the AASHO Road Test showed that lateral movement of material in the subbase accounted for most of the rutting observed (Ref 10). The excessive traffic consolidation in the upper portion of the pavement and the plastic deformation due to insufficient mix stability are claimed as the primary cause of pavement rutting in Western states (Ref 11).

To minimize surface rutting, Shell Company engineers used results from the AASHO Road Test to develop a compressive strain criteria equation (Ref 12):

$$W_{18} = 6.15 \times 10^{17} \left(\frac{1}{\epsilon_c}\right)^{4.0} \tag{3.3}$$

where ϵ_c is the compressive microstrain at the top of the subgrade, and W_{18} is the number of weighted 18-kip axle loads prior to excessive permanent deformation.

PRESENTATION AND DISCUSSION OF RESULTS

Effect of Tire Inflation Pressure and Axle Load on Surface Tensile Strain

To demonstrate the accuracy of the TEXGAP-3D finite element modeling, results were compared to a layer program (ELSYM5) for a uniform circular pressure model. Figure 3.3 shows the comparison between the 3D uniform pressure model (TEXGAP-3D) and the uniform circular pressure model (ELSYM5) for the tensile strain at bottom of the surface with various surface thicknesses (Note that the U designates the uniform pressure model by employing TEXGAP-3D, and that the L designates the results from layer program ELSYM5). There is a close correspondence between the results from the two models. The increase in tire inflation pressure from 75 psi to 110 psi (a 47% increase) results in an approximate 102 microstrain increase (a 65% increase) at the bottom of a 1.50-inch-thick surface pavement. For thicker surface pavements, the effect of the tire-pavement contact pressure distribution on the surface tensile strain becomes less significant.

Figure 3.4 shows a comparison between the experimental nonuniform pressure model and the uniform pressure model for the tensile strain at the bottom of the surface with various surface thicknesses (T designates the treaded tire experimental contact pressure model). With a 47% increase in tire inflation pressure, the uniform pressure model predicts a 62% increase in the surface tensile strain at the bottom of the 1.5-inch-thick pavement, while the experimental model yields a 33% increase in surface tensile strain. The uniform pressure model overestimates the reduction in contact area with increased tire inflation pressure (from 75 psi to 110 psi). For example, with the 47% increase in tire inflation pressure, the uniform pressure model will produce a 32% decrease in contact area, as

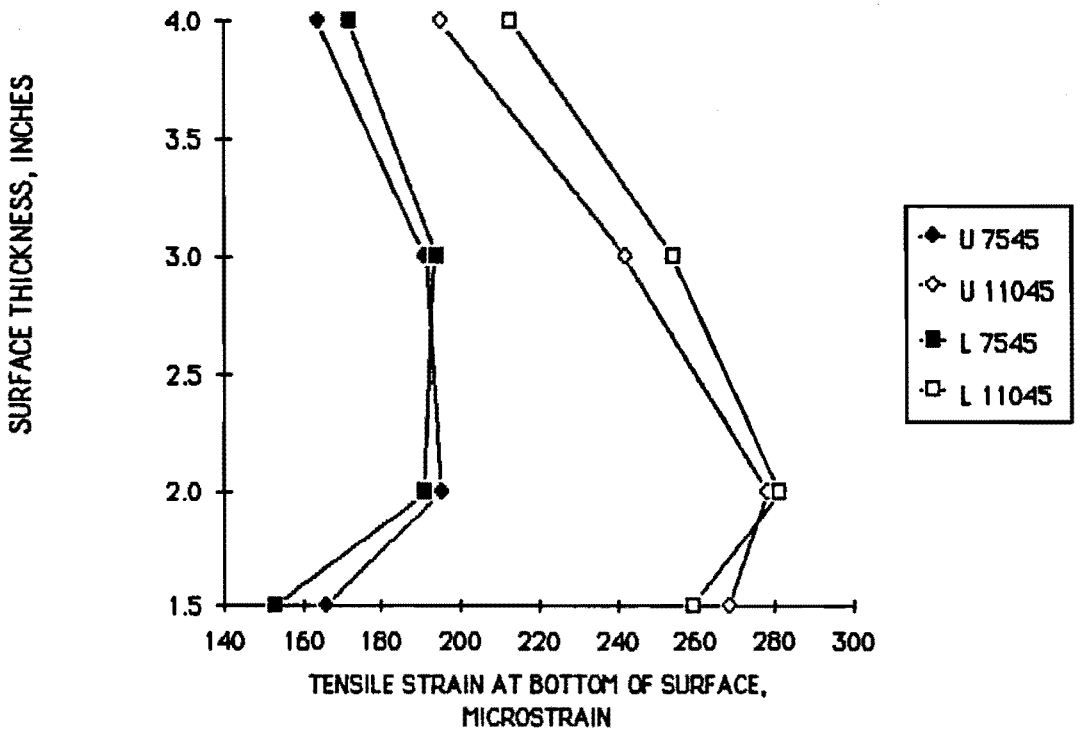

Fig. 3.3 Effect of pressure distribution model on critical tensile strain at the bottom of the surface

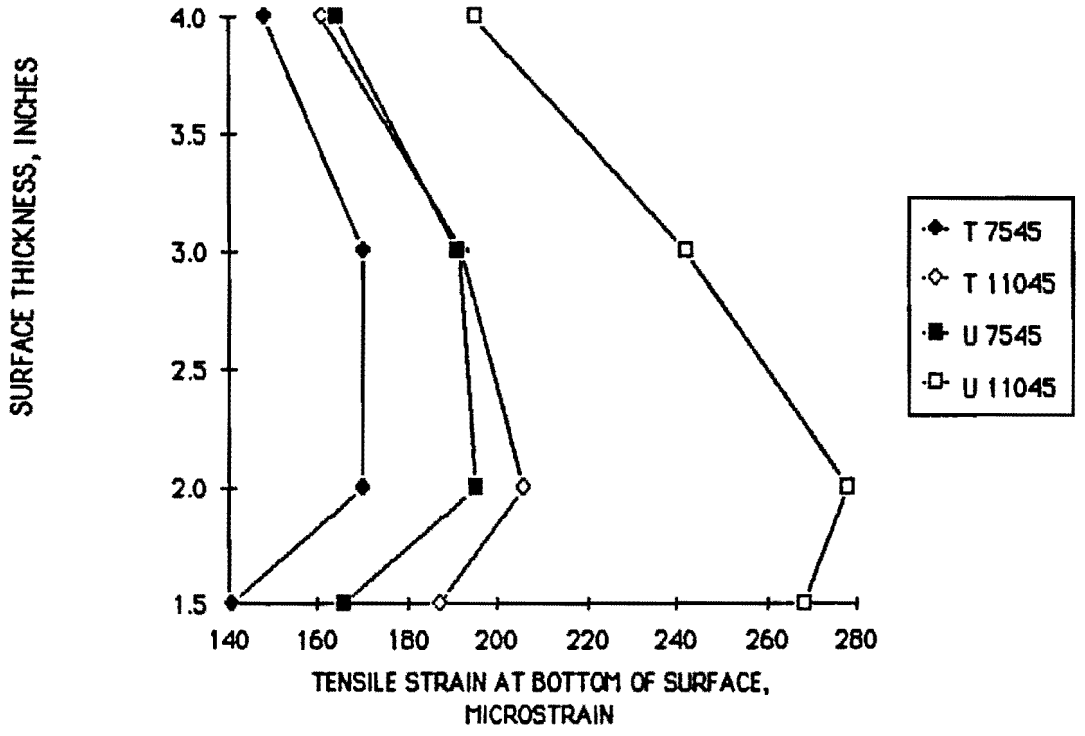

Fig. 3.4 Effect of inflation pressure on the critical tensile strain at the bottom of the surface

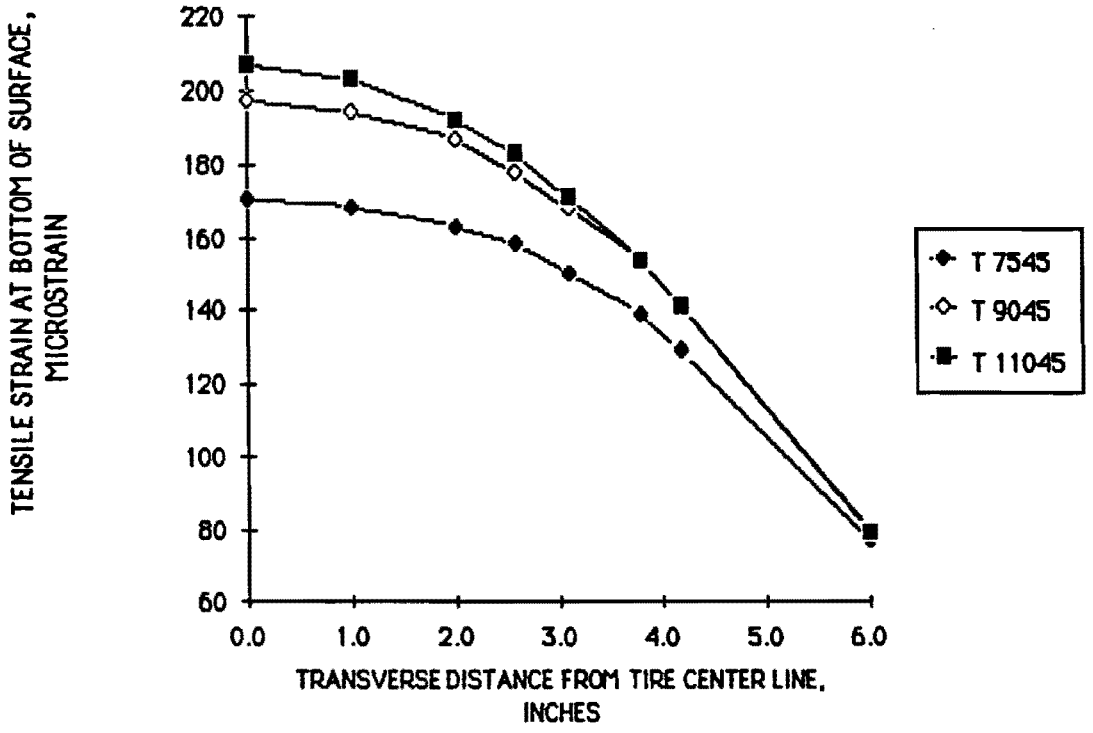

Fig. 3.5 Effect of inflation pressure on the tensile strain contour at the bottom of a 2-inch-thick surface pavement

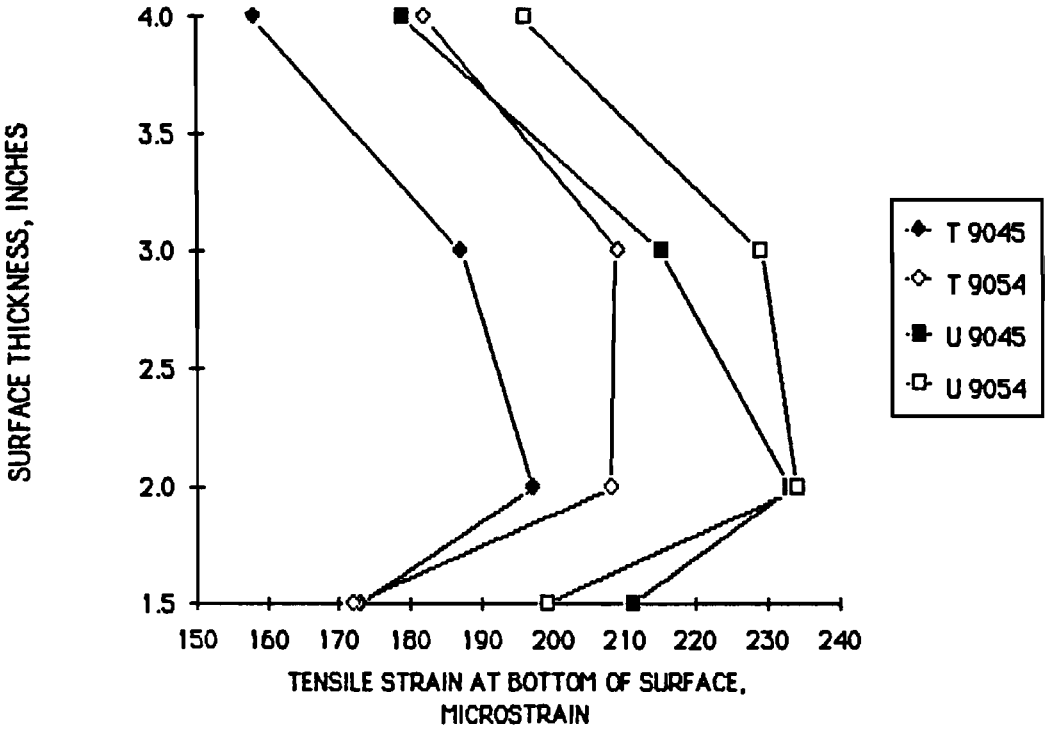

Fig. 3.6 Effect of axle load on the tensile strain at the bottom of the surface

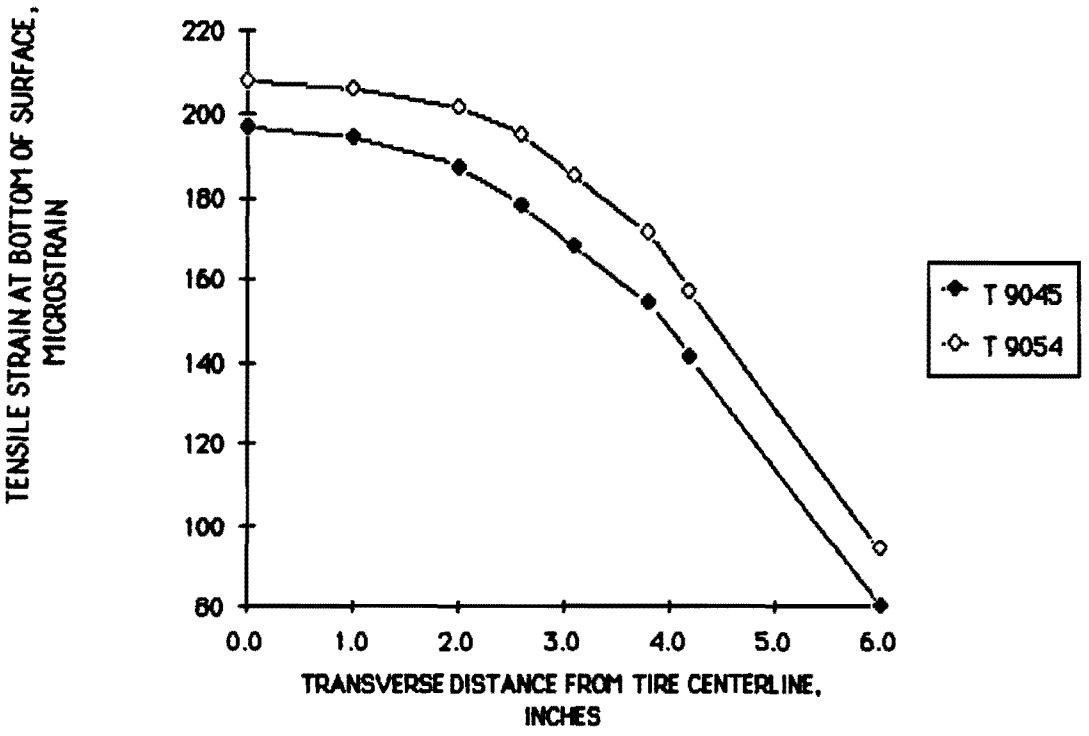

3.7 Effect of axle load on the tensile strain at the bottom of a 2-inch-thick surface pavement

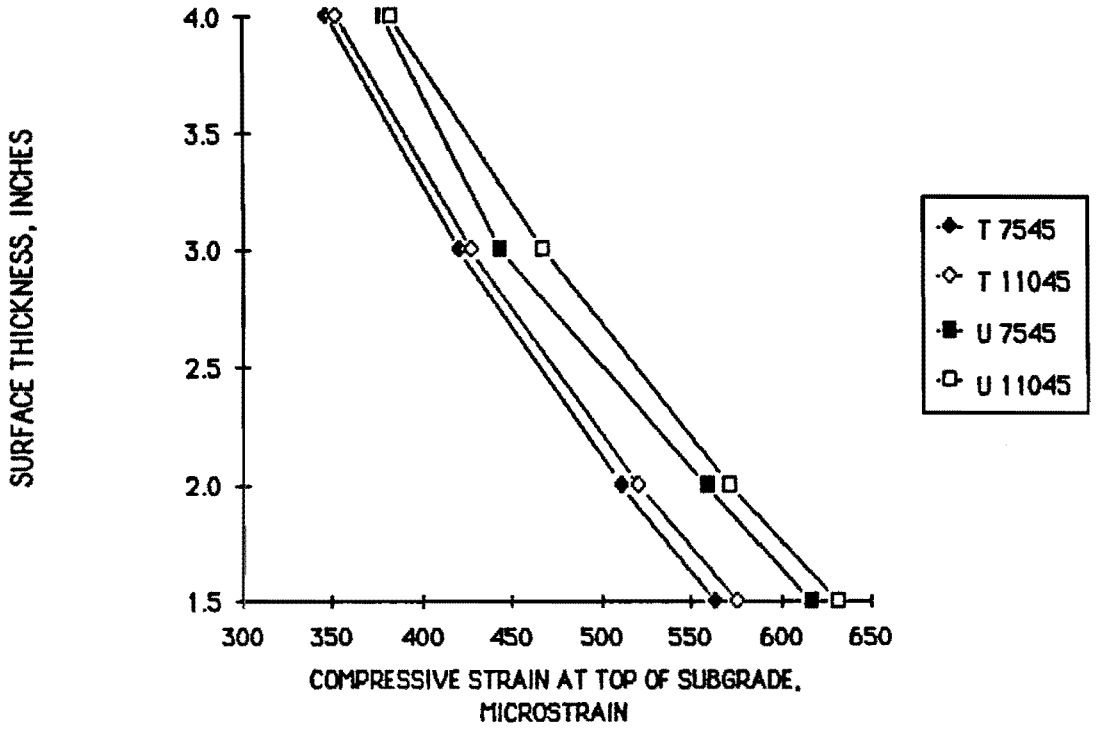

Fig. 3.8 Effect of inflation pressure on the compressive strain at the top of the subgrade

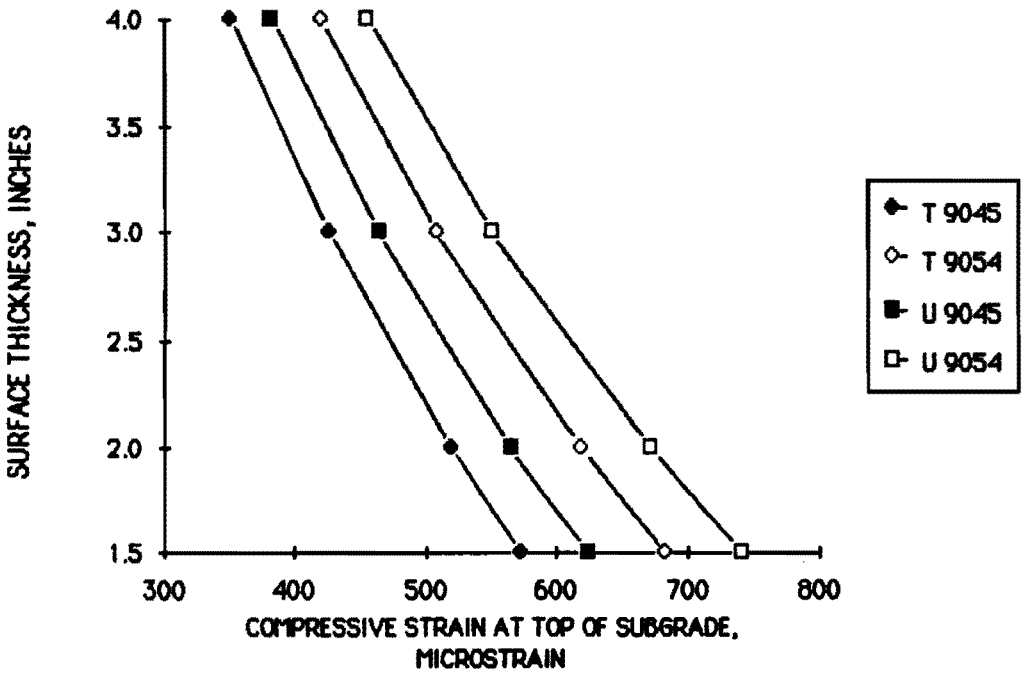

3.9 Effect of axle load on the compressive strain at the top of the subgrade

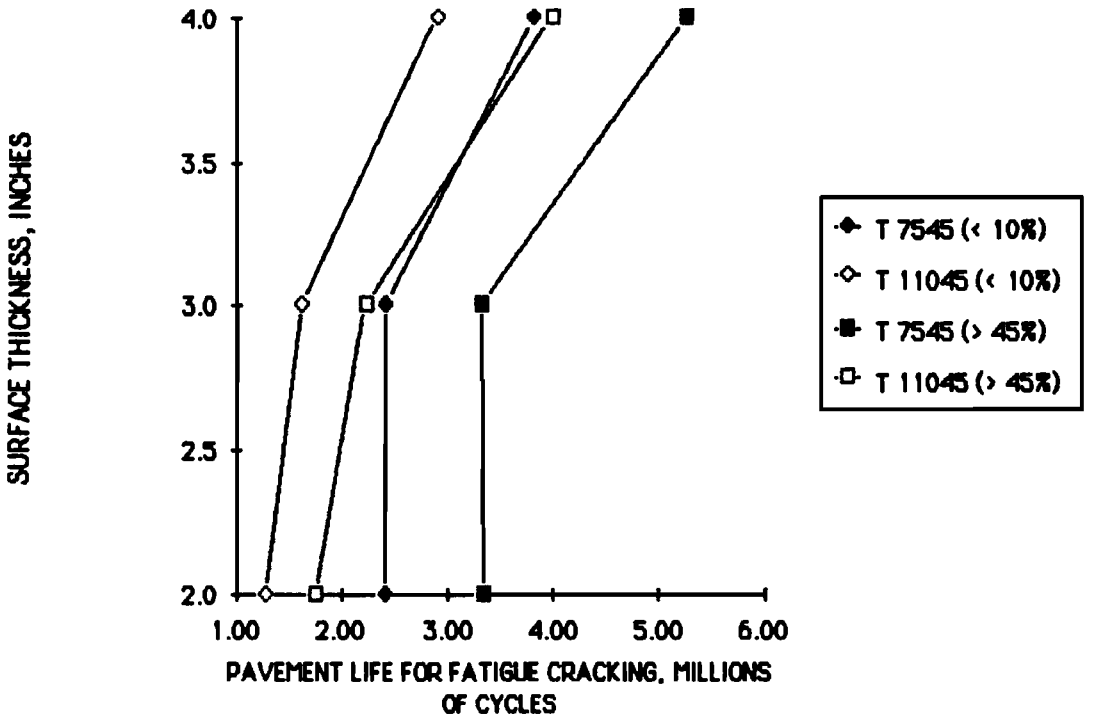

3.10 Effect of inflation pressure on the pavement fatigue damage life

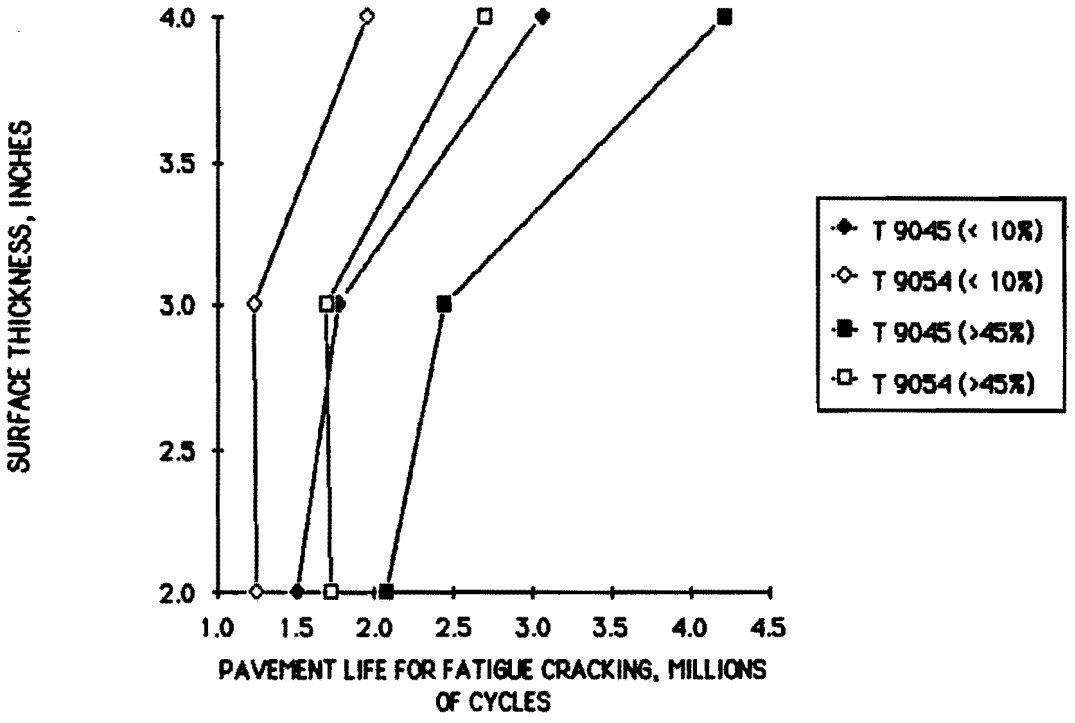

3.11 Effect of axle load on the pavement fatigue damage life

compared to a measured 9% decrease in truck tire gross contact area.

Figure 3.5 shows the effect of increased tire inflation pressure on the tensile strain at the bottom of the surface layer for a 2-inch-thick surface. The tensile strain is shown along the tire transverse direction. At a distance of 6 inches from the tire center line, the inflation pressure will have no significant effect on the surface tensile strain.

Figure 3.6 shows the effect of tire axle load on critical tensile strain for surface thicknesses of from 1.5 to 4 inches for both the nonuniform experimental pressure model and the uniform pressure model. The results from the uniform pressure model are conservative in comparision to the experimental model for the surface thicknesses considered. As anticipated, the overloaded tire consistently produces the highest strains. For the 4-inch-thick surface pavement and a 20% increase in the axle load, the uniform pressure model results in a 10% increase in the surface tensile strain as compared to a 15% increase for the experimental pressure model. The uniform pressure model overestimates the increase in contact area with increasing axle load, and therefore the model produces a smaller increase in surface tensile strain.

Figure 3.7 shows the tensile strain developed at the bottom of the 2-inch-thick surface course by applying a 4500-lbf load and a 5400-lbf load (20% overload) to the treaded tire at the rated inflation pressure of 90 psi. The overloaded tire consistently produces a higher tensile strain, even at a distance of 6.0 inches from the tire center line.

Effect of Tire Inflation Pressure and Axle Load on Subgrade Compressive Strain

Figure 3.8 shows that a 47% increase in inflation pressure produces less than a 2% increase in the compressive strain developed at the top of the subgrade for both the uniform pressure model and the nonuniform experimental pressure model. The uniform pressure model consistently overestimated the subgrade compressive strain except for thick surface pavements.

From Fig 3.9, it can be seen that the axle load has a significant effect on the compressive strains at the top of the subgrade for both the uniform pressure model and the nonuniform pressure model. The figure shows that a 20% increase in axle load produces an approximately 20% increase in the critical subgrade compressive strain for both models. However, the uniform pressure model consistently overestimated the subgrade compressive strain for the full range of surface thicknesses.

Effect of Tire Inflation Pressure and Axle Load on Fatigue Cracking Life

The number of loads of constant stress necessary to cause fatigue cracking can be obtained by substituting the computed tensile strain from finite element program TEXGAP-3D into Eq 3.1 and Eq 3.2 for either the 10% cracking model or the 45% cracking model. Figure 3.10 shows the effect of increased tire inflation pressure on fatigue damage life for various surface thicknesses. The pavement life improves with thicker pavements. For the 2-inch-thick surface pavement, a 47% increase in tire inflation pressure results in a 22% increase in surface tensile strain and therefore, a 48% reduction of the pavement life for both the 10% fatigue cracking model and the 45% fatigue cracking model.

Figure 3.11 shows the effect of truck tire overload on pavement fatigue life for various surface thicknesses (2 to 4 inches). For a 4-inch surface pavement, a 20% increase in axle load will cause a 36% reduction in pavement life for both fatigue cracking models. The tensile strains at the bottom of the surface and the corresponding number of constant stress cycles (N_f) necessary to cause either 10% or 45% fatigue cracking are given in Table 3.1 for various surface thicknesses, tire inflation pressures, and axle loads.

TABLE 3.1 THE TENSILE STRAIN AT THE BOTTOM OF THE SURFACE AND THE CORRESPONDING FATIGUE LIFE FOR VARIOUS SURFACE THICKNESSES, INFLATION PRESSURES, AND AXLE LOADS

	Tensile Strain at Bottom of Surface (microstrain)			10% Fatigue Cracking Model (million cycles)			45% Fatigue Cracking Model (million cycles)		
Surface Thickness (inches)	2.0	3.0	4.0	2.0	3.0	4.0	2.0	3.0	4.0
T7545	170.0	170.4	148.1	2.42	2.40	3.82	3.34	3.31	5.26
T11045	206.5	192.3	161	1.27	1.62	2.90	1.76	2.23	3.99
T9045	196.5	187	158.4	1.51	1.77	3.06	2.07	2.44	4.21
T9054	208	208.9	181.6	1.25	1.23	1.95	1.72	1.69	2.69
U7545	194.6	191.1	163.8	1.55	1.65	2.74	2.14	2.27	3.77
U11045	277.8	242	194.5	0.48	0.76	1.56	0.66	1.04	2.14
U9045	232.6	214.8	178.6	0.864	1.12	2.06	1.19	1.55	2.84
U9054	233.6	228.8	196.5	0.85	0.91	1.50	1.17	1.26	2.07

Note: T designates a treaded tire, with a nonuniform (experimental) pressure model, and U designates a uniform pressure model. The last two digits (45 and 54) stand for 4500 lbf and 5400 lbf respectively, and the number (75, 90, and 110) represents the inflation pressure at 75 psi, 90 psi, and 110 psi respectively; i.e., T7545 is a treaded tire, with a 75 psi inflation pressure and a 4500 lbf axle load; and U7545 is a uniform pressure model, with a 75 psi inflation pressure and a 4500 lbf axle load.

Effect of Axle Load on Subgrade Rutting Life

Figure 3.12 shows the effect of increased axle load on the subgrade rutting damage life for various surface thicknesses. A 20% increase in axle load will result in a 19% increase in subgrade compressive strain and a 50% reduction in pavement life. The subgrade compressive strains and the corresponding rutting lives for various surface thicknesses, inflation pressures, and tire axle loads are given in Table 3.2.

SUMMARY

The effects of high tire inflation pressure and heavy axle load on asphalt concrete pavement stresses and strains (and the corresponding pavement damage life) were analyzed using the 3D finite element tire-pavement contact pressure model rather than the uniform circular pressure model or the nonuniform concentric circular pressure model. Table 3.3 shows a comparison between the 3D finite element model (uniform or nonuniform pressure distribution) TEXGAP-3D and ELSYM5. It can be concluded that the uniform pressure model overestimates the tensile strain at the bottom of the surface for either the underinflated or overinflated tire. The uniform pressure model will predict a higher percent increase in tensile strain than the nonuniform experimental pressure model. However, with the same percent increase in truck tire axle load, the uniform pressure model will underestimate the percent increase in the surface tensile strain.

The effects of increased tire inflation pressure on the tensile strains at the bottom of the surface are greatest for surface thickness less than 2 inches. A 47% increase in the tire inflation pressure results in a 33 % increase in tensile strains at the bottom of the surface and a 60% reduction in fatigue cracking life. The axle load also has a significant effect on the tensile strains at the bottom of the surface layer. A 20% increase in the tire axle load will result in a 15% increase in tensile strain and a 36% reduction in fatigue cracking life.

The tire inflation pressure will have less than a 2% effect on the compressive strains at the top of the subgrade for either the uniform pressure model or the nonuniform pressure model. Therefore, inflation pressure is an insignificant factor in causing subgrade rutting.

The axle load has a significant effect on the subgrade compressive strain and the corresponding subgrade rutting life. A 20% increase in axle load results in a 19% increase in subgrade compressive strain and a 50% (approximate) reduction of the pavement life.

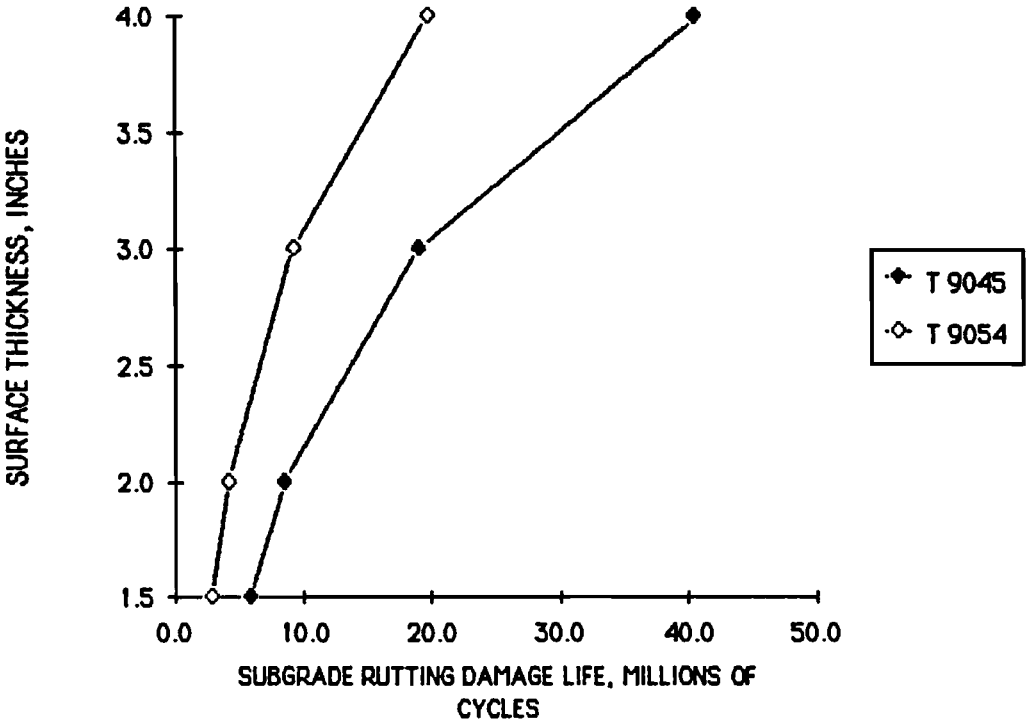

Fig. 3.12 Effect of axle load on the pavement subgrade rutting damage life

TABLE 3.2 THE COMPRESSIVE STRAIN AT THE TOP OF THE SUBGRADE AND THE CORRESPONDING PAVEMENT DAMAGE LIFE FOR VARIOUS SURFACE THICKNESSES, INFLATION PRESSURES, AND AXLE LOADS

	Compressive Strain at Top of Subgrade (microstrain)				Million Load Cycles Prior to Excessive Deformation (rutting)			
Surface Thickness (inches)	1.5	2.0	3.0	4.0	1.5	2.0	3.0	4.0
T7545	562.8	510.8	419.6	347.2	6.13	9.03	19.8	42.3
T11045	575.3	521.4	427.2	352.6	5.61	8.32	18.5	39.8
T9045	571	518	424.7	351	5.78	8.54	18.9	40.5
T9054	681	618.3	508	420.4	2.86	4.21	9.23	19.7

TABLE 3.3 COMPARISON OF VARIOUS MODELS FOR TENSILE STRAIN AND SUBGRADE COMPRESSIVE STRAIN

	47% Increase in the Tire Inflation Pressure			20% Increase in the Truck Tire Axle Load		
	Non Uniform	Uniform	ELSYM5	Non Uniform	Uniform	ELSYM5
Tensile Strain at Bottom of Surface (% increase)	33	62	69	15	10	8
Subgrade Compressive Strain (% increase)	2	2	5	19	19	17

CHAPTER 4. RIGID PAVEMENT ANALYSIS

Rigid pavements are designed to carry tire loads in a way, different than flexible pavements, since rigid pavement performance depends on resistance to bending. Rigid pavement is analysed as a beam supported on an elastic foundation. A rigid pavement generally consists of a Portland cement slab on a compacted subgrade. Since the modulus of elasticity of the concrete slab is much greater than that of the foundation material, a major portion of the load-carrying capacity is derived from the slab itself. Base courses are used when additional load capacity is desired or when the native soil exhibits undesirable drainage characteristics. Stresses in rigid pavements depend on total tire load, tire inflation pressure, the spacing of multiple wheels, the position of loading on the pavement (corner or interior), and the subgrade support (Ref 7).

The objective of this chapter is to determine the effect of pressure distribution (uniform model versus nonuniform experimental pressure model) on the maximum tensile stress at the bottom of a concrete slab. The pavement description and the computer models used in the analysis of the rigid pavement are described.

RIGID PAVEMENT MODEL

A rigid pavement is modeled as a two layer system resting on a Winkler foundation in the computer program JSLAB (Ref 13). Material properties and slab dimensions are shown in Fig 4.1. The slab size is 15 feet long and 12 feet wide. The frictional condition is assumed to exist between adjacent layers. The maximum horizontal (edge) stress at the bottom of the slab is the desired output variable.

DESCRIPTION OF PROGRAM JSLAB

The finite element program JSLAB can analyze concrete pavement sections consisting of up to nine slabs. The program can analyze a one or two layer pavement system resting on a Winkler foundation. The two layers may be unbonded or fully bonded. Permissible loadings include wheel loads at any location on the slab, nodal point forces, nodal displacements, and tire pressure. A more detailed description of JSLAB is given in (Ref 13).

The computer program JSLAB is used in this study to show what effect different input pressure distribution models have on the tensile stress at the bottom of the slab where the tensile stress is maximum. This is the critical stress for a rigid pavement (provided the material is relatively homogeneous and contains no stress concentrations).

PRESSURE DISTRIBUTION MODEL FOR JSLAB

The form of input used by JSLAB is an array of experimental contact pressures (inflation pressure of 110 psi and axle load of 4500 lbf) acting at specific locations in the tire footprint (see Table 4.1 and Fig 4.2). The program JSLAB allows the user to apply the tire load anywhere on the slab. This permits a "worst case" analysis to be performed, as when one single tire axle load is applied at the left hand corner of the slab.

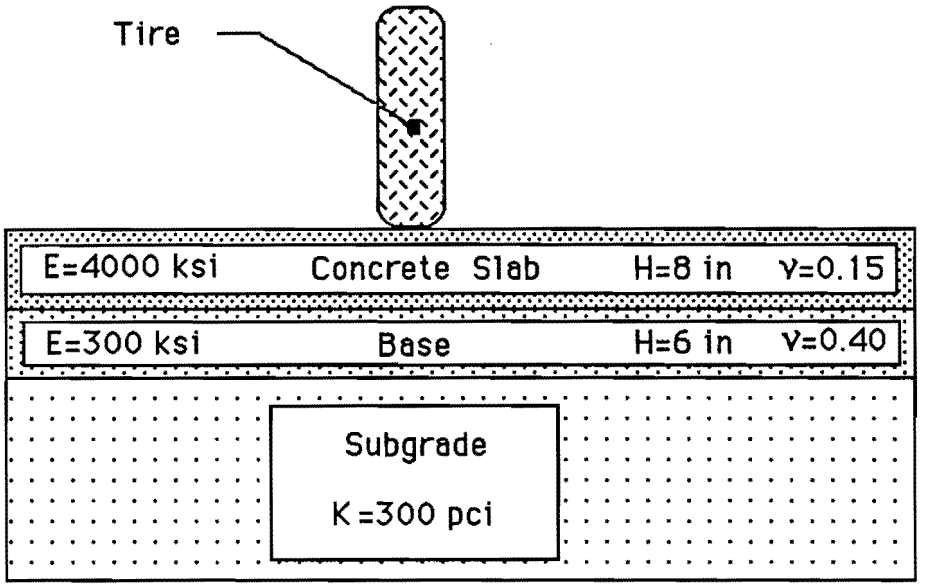

Fig 4.1. Rigid pavement diagram and parameter values used in JSLAB

TABLE 4.1 PRESSURE ARRAY USED IN COMPUTER PROGRAM JSLAB

76	86	99	112
104	112	124	156
117	114	112	143
126	134	119	151
133	118	125	147
91	99	113	141
79	89	88	96

94	85	99
113	97	103
105	88	119
109	103	105
115	91	108
105	90	107
104	87	100

105	98	87	79
140	114	127	116
129	122	142	125
143	130	140	152
129	115	151	132
133	111	107	103
96	85	97	81

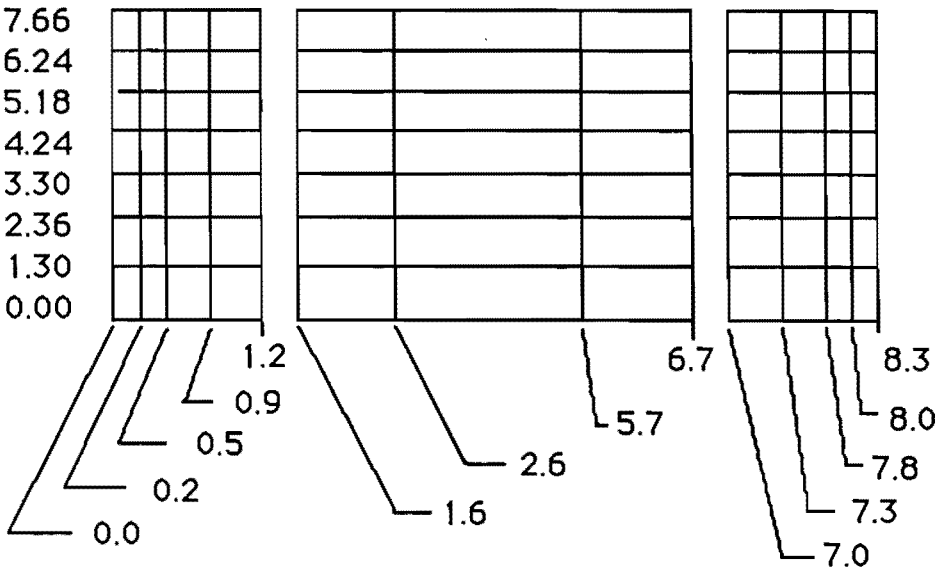

Fig 4.2. Grid spacing used in JSLAB (dimensions in inches)

PRESENTATION AND DISCUSSION OF RESULTS

Figure 4.3 shows the edge stress at the bottom of the slab versus the distance along the wheel path for the case of (1) the treaded tire at a 4500 lbf load and (2) the uniform pressure model, both at a 110-psi inflation pressure. The tensile stress at the bottom along the critical edge of the slab for both cases is almost identical. Although not shown in this report, only the axle load (not the tire inflation pressure) affects the magnitudes of the stresses developed in a rigid pavement in response to tire loads.

SUMMARY

Based on the limited number of contact pressure distributions and pavements studied in this chapter, it was found that the uniform pressure model gave almost identical results (when compared with the experimental model) for predicting the tensile stresses at the bottom of the slab. This indicates that the pressure distribution model (for the same tire axle load) has little effect on rigid pavement performance.

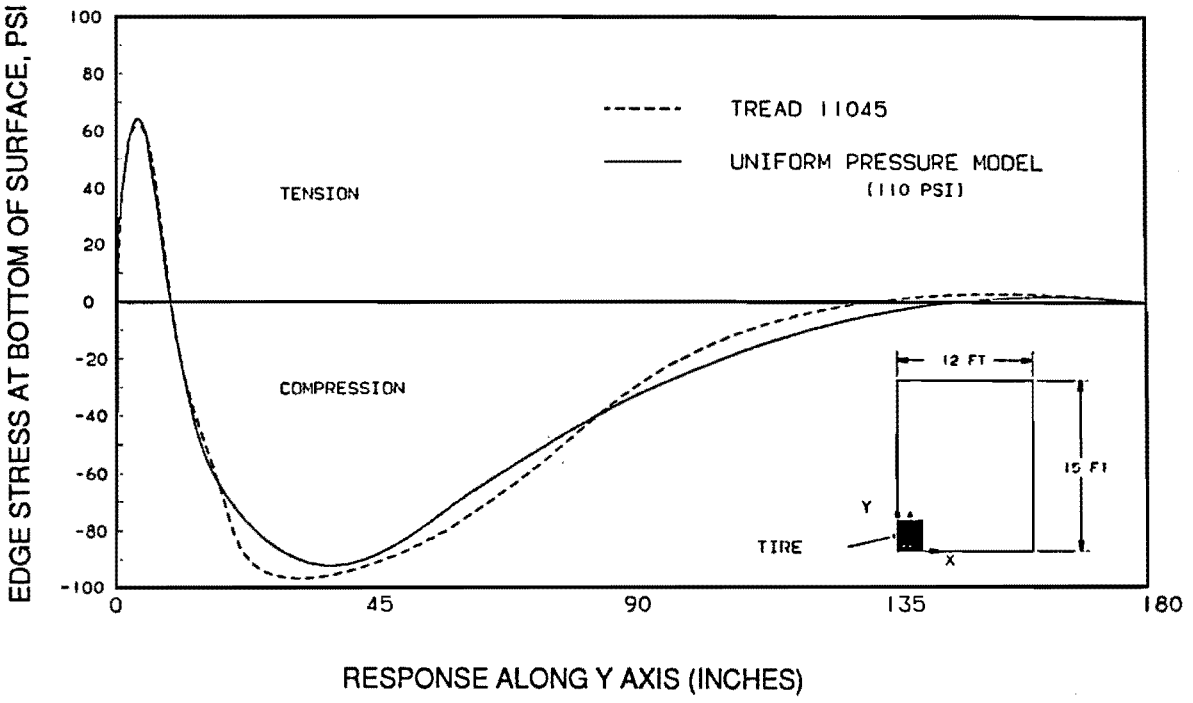

Fig 4.3 Effect of inflation pressure on tensile stresses in concrete slab

CHAPTER 5. CONCLUSIONS AND RECOMMENDATIONS

This chapter summarizes the contributions of this research. Recommendations for future research are also presented.

SUMMARY OF WORK ACCOMPLISHED

The main contribution of this report is the determination of the effects of high inflation pressures and heavy axle loads on flexible pavement performance by using an experimental nonuniform pressure model instead of a uniform circular pressure model, which is commonly used for pavement design. The tensile strain at the bottom of the surface (which is associated with fatigue cracking) and the compressive strain at the top of the subgrade (which is associated with rutting) are obtained for various surface thicknesses, inflation pressures (75 psi, 90 psi, and 110 psi), and axle loads (4500 lbf and 5400 lbf) by employing the layer programs (BISAR and ELSYM5), and the 3D finite element program (TEXGAP-3D). The rigid pavement analysis was conducted with both an experimental nonuniform pressure model and a uniform pressure model as input to the program JSLAB.

CONCLUSIONS

The conclusions presented in this report show the effect of braking force, tread type, inflation pressure, axle load, pressure distribution model, and pavement surface thickness on pavement performance.

Braking Force Effect

Superimposing a tangential force (as with braking vehicles) onto the normal load does not significantly affect the critical tensile strain for high modulus and thick surface pavements. However, for thin and flexible (low modulus) pavements, the stress distribution is quite different from that obtained using only normal force loading.

Tread Type Effect

The tread type has little effect on the critical tensile strain at the bottom of a 4-inch-thick surface course pavement, and it likewise has little effect on the strains produced at the top of the subgrade. However, for thin and low modulus flexible pavements, the high contact pressures near the tire shoulder region produce a critical tensile strain at a radial distance of 2.5 inches from the tire center line.

Tire Inflation Pressure Effect

(1) For thin and flexible pavements, an underinflated tire will produce a maximum strain under the tire shoulder while an overinflated tire will produce a maximum strain beneath the center of the tire.
(2) Increasing the truck tire inflation pressure will produce a significant increase in the tensile strain

at the bottom of the surface and therefore a significant decrease in the fatigue damage life. For example (for the 2-inch-thick surface pavement) a 47% increase in the tire inflation pressure results in a 33% increase in the surface tensile strain and, therefore, a 48% reduction in pavement life for both the 10% fatigue cracking model and the 45% fatigue cracking model. The pavement life improves with thicker pavements.

(3) The inflation pressure will have a minimal effect on the compressive strains developed at the top of the subgrade, especially for pavements with thick bases.

Axle Load Effect

(1) A heavy axle load produces a high truck tire contact pressure distribution (between the tire shoulder and circumferential gap) which will produce significant increases in the tensile strain at the bottom of the thin surface course, with the maximum strains occuring below the high contact pressure regions.

(2) The axle load plays a significant role in causing fatigue cracking and subgrade rutting. For example (for a 4-inch-thick surface pavement), a 20% increase in axle load will cause a 36% reduction in fatigue pavement life and a 50% reduction in subgrade rutting life.

Effect of Pressure Distribution Model

(1) Experimental results show that the truck tire shoulder regions produce two strips of high contact pressures which can dominate the whole contact pressure distribution. Therefore, the 3D finite element pressure model appears to be the best model, as compared with the nonuniform circular pressure model for analyzing flexible pavement performance.

(2) The uniform pressure model overestimates the increase in tensile strain at the bottom of the surface for overinflated tires, and underestimates the increase in tensile strain at the bottom of the surface for overloaded tires. For example, with a 47% increase in the tire inflation pressure, the uniform pressure model will predict a 62% increase in surface tensile strain as compared to a 33% increase for the experimental nonuniform pressure model.

(3) The uniform pressure model overestimates the surface tensile strain and the subgrade compressive strain for both the overinflated and underinflated tires.

(4) For the rigid pavement, the effect of the pressure distribution model on the surface tensile stress is minimal.

Surface Thickness Effect

(1) In general, for pavments of between 1 inch and 4 inches, the thicker the surface pavement, the greater the pavement damage life.

(2) For heavy traffic, surface thicknesses of between 1 and 3 inches should be avoided for most cases since typical material combinations do not provide adequate pavement life. A realistic surface thickness should be at least 4 inches thick for most applications.

RECOMMENDATIONS

Based on the analysis conducted in this study, the following recommendations are made:

(1) An analysis should be performed to compare the effect of radial versus bias-ply tires on flexible pavement performance.

(2) A 3D finite element model pressure distribution appears to be the best representation of the tire-pavement interaction. However, for the TEXGAP-3D program, the number of 3D solid elements is limited. Another general purpose finite element program with greater computing capacity (NASTRAN, ANSYS) should be used to determine pavement stresses for dual wheel pressure distributions and for pavement models with more than three layers.
(3) A mathematical model should be developed to predict rutting in asphalt concrete pavements exposed to future truck traffic, which will involve high tire inflation pressure and high traffic volume.
(4) Flexible surface deformations should be measured and compared with the results from a 3D finite element analysis in order to validate the analysis.

REFERENCES

1. Marshek, K. M., Hudson, W. R., Connell, R. B., Chen, H. H., and Saraf, C. L., "Experimental Investigation of Truck Tire Inflation Pressure on Pavement-Tire Contact Area and Pressure Distribution" Research Report 386-1, Center for Transportation Research, The University of Texas at Austin, 1985.

2. Love, A. E. H., "The Stress Produced on a Semi-Infinite Body by Pressure on Part of the Boundary," Philosophical Transaction of the Royal Society, Series A, Vol. 228, 1929.

3. Burmister, D. M., "Theory of Stresses and Displacements in Layered Systems," Proceedings, Highway Research Board, Vol. 23, Washington, D. C., pp. 126-148, 1943.

4. Duncan, J. M., Monismith, C. L., and Wilson, E. L., "Finite Element Analysis of Pavements," Highway Research Record, Vol. 228, Highway Research Board, Washington, D. C. 1968.

5. BISAR, Computer Program User's Manual. Amsterdam: Koninklijke/Shell-Laboratorium, 1972.

6. Clark, Samuel K., Editor. Mechanics of Pneumatic Tires. Washington,D.C. : U.S. Department of Transportation, 1975.

7. Yoder, E.J., and M.W. Witczak. Principles of Pavement Design. New York: John Wiley and Sons, Inc., 1975.

8. Woods, Kenneth B., Editor. Highway Engineering Handbook. New York: McGraw-Hill, 1960.

9. Finn, F., Saraf, C., Kulkarni, R. et al, "The Use of Distress Prediction Subsystems for the Design of Pavement Structures," Proceedings, Fourth International Conference on the Structural Design of Asphalt Pavements, Ann Arbor, Michigan, 1977.

10. The AASHO Road Test: Report 5, Pavement Research, Highway Research Board Special Report 61E, National Academy of Science, Washington, D. C., 1962.

11. Shell International Petroleum Company Limited, Shell Pavement Design Manual, London, 1978.

12. Betenson, W. B., Hanson, D. I., Jones, W. C., Mayruth, J. J., Warburton, R. G., "Asphalt Pavement Rutting-Western States," FHWA/TS-84/211, Western Association of State Highways and Transportation Officials, 1984.

13. Tayabji, Shiraz D., and Bert E. Colley. Analysis of Jointed Concrete Pavements. Skokie, Ill.: Portland Cement Association, 1981.

APPENDIX A

NONUNIFORM CIRCULAR PRESSURE MODEL FOR PROGRAM BISAR

APPENDIX A: NONUNIFORM CIRCULAR PRESSURE MODEL FOR PROGRAM BISAR

Experimental nonuniform circular pressure models for a treaded tire with various inflation pressures (75 psi, 90 psi, and 110 psi) and an axle load of 4500 lbf are respectively plotted in Figs. A.1, A.2, and A.3. The pressure distribution model for a 90 psi inflation pressure and a 5400 lbf axle load is plotted in Fig. A.4. Nonuniform pressure models for a bald tire (75 psi and 110 psi and 4500 lbf) are, respectively, plotted in Figures A.5 and A.6

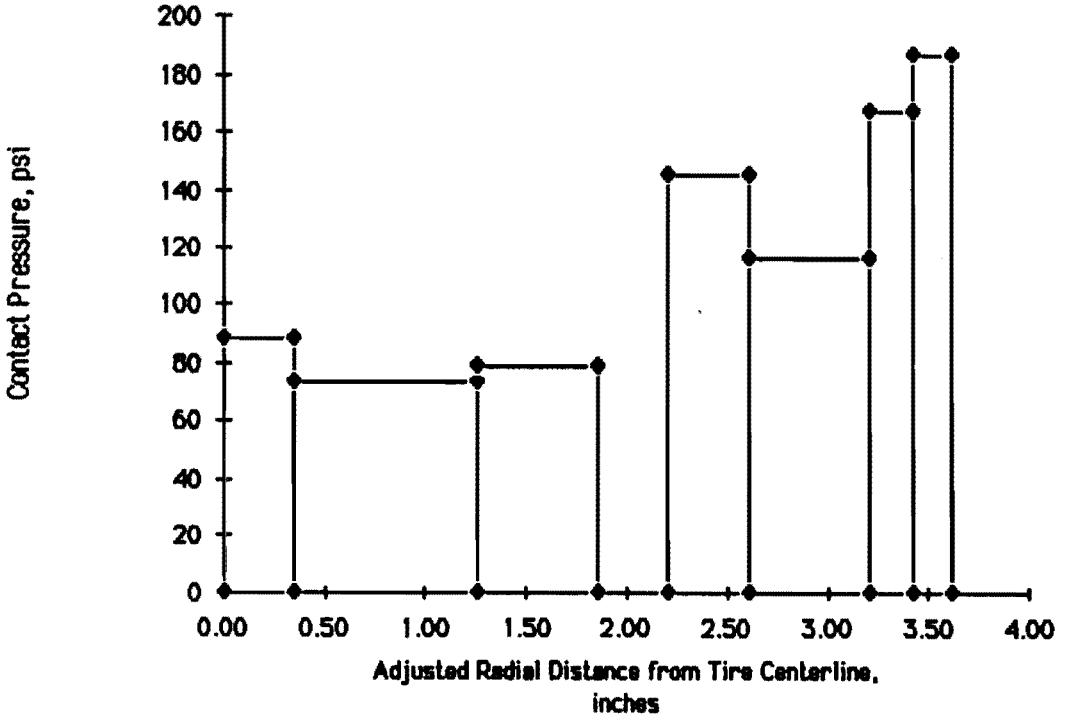

Fig. A.1 Nonuniform pressure model for a treaded tire with an inflation pressure of 75 psi and an axle load of 4500 lbf

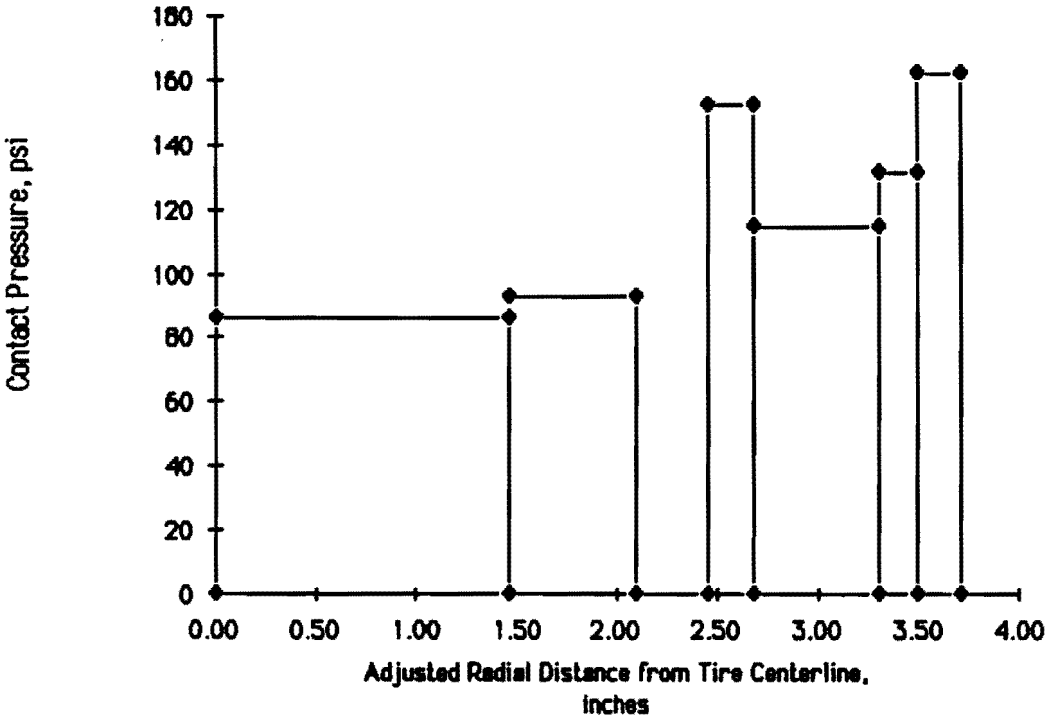

Fig. A.2 Nonuniform pressure model for a treaded tire with an inflation pressure of 90 psi and an axle load of 4500 lbf

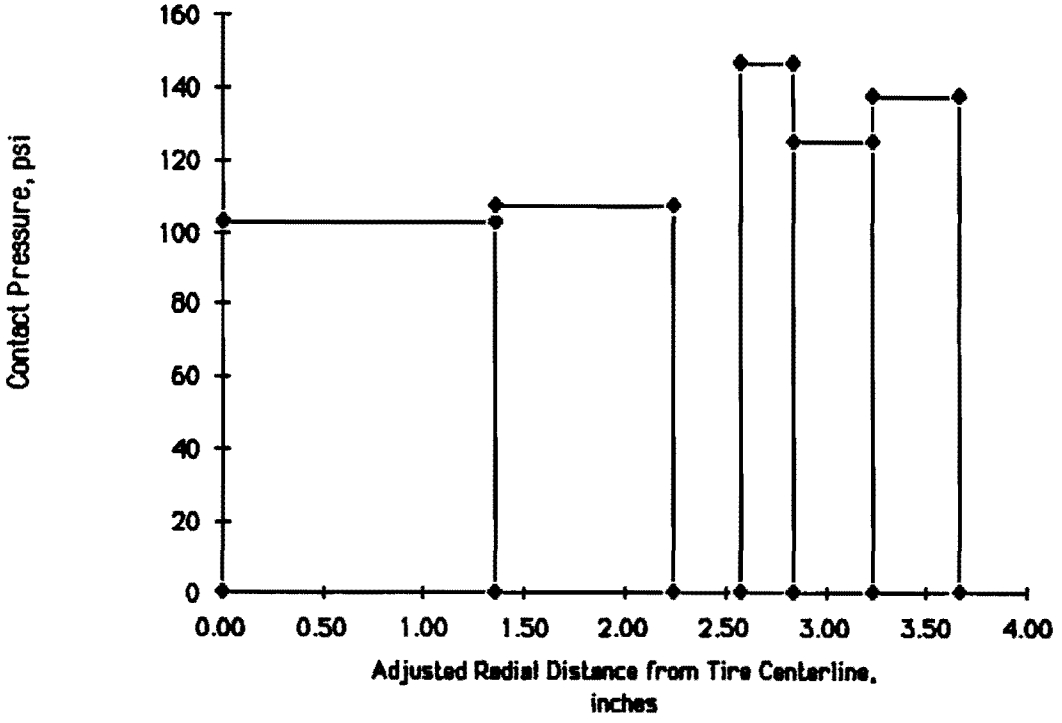

Fig. A.3 Nonuniform pressure model for a treaded tire with an inflation pressure of 110 psi and an axle load of 4500 lbf

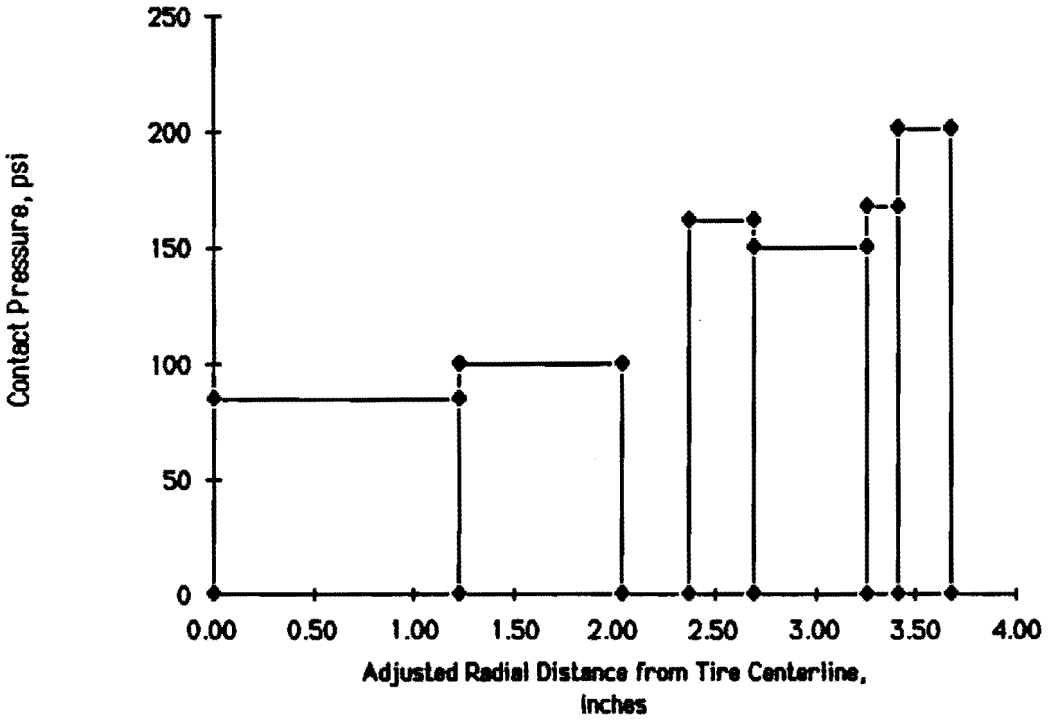

Fig. A.4 Nonuniform pressure model for a treaded tire with an inflation pressure of 90 psi and an axle load of 5400 lbf

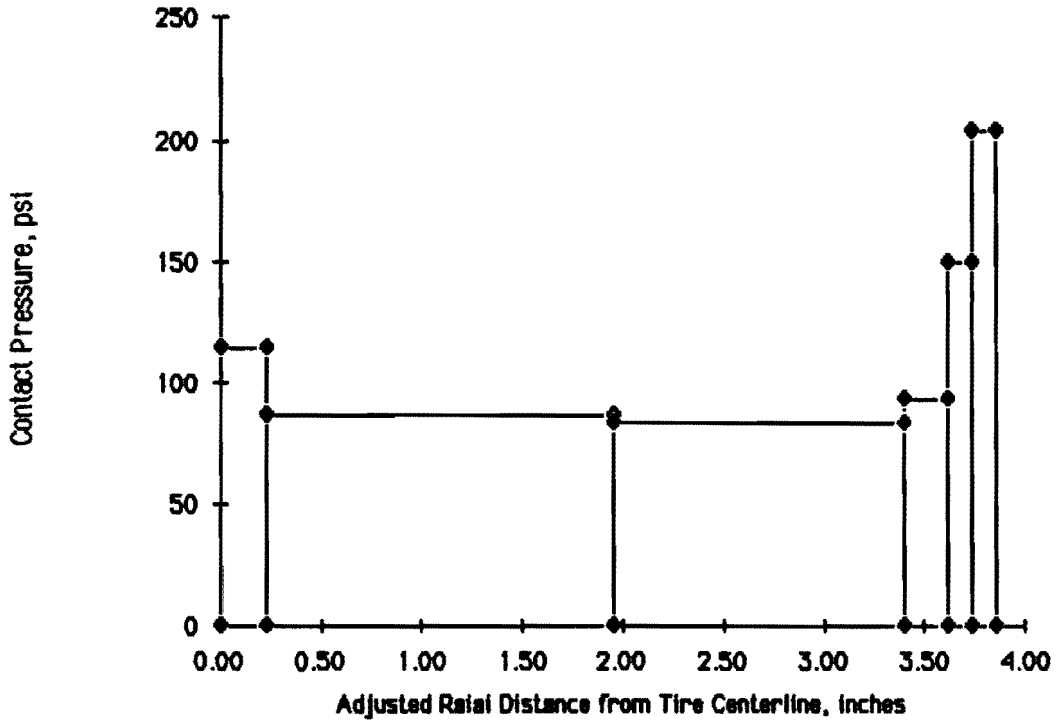

Fig. A.5 Nonuniform pressure model for a bald tire with an inflation pressure of 75 psi and an axle load of 4500 lbf

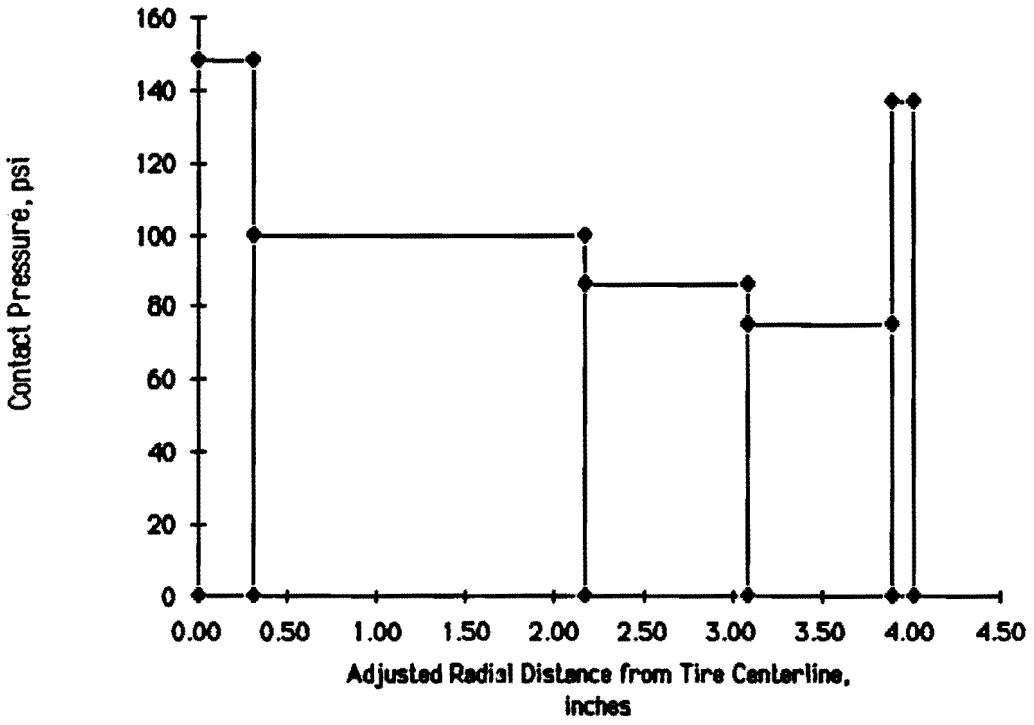

Fig. A.6 Nonuniform pressure model for a bald tire with an inflation pressure of 110 psi and an axle load of 4500 lbf

APPENDIX B

NONUNIFORM 3D PRESSURE MODEL FOR PROGRAM TEXGAP-3D

APPENDIX B: 3D PRESSURE MODEL FOR PROGRAM TEXGAP-3D

The 3D experimental nonuniform pressure models for various inflation pressures (75 psi, 90 psi, and 110 psi) and an axle load of 4500 lbf are given respectively in Tables B.1, B.2, and B.3. The pressure distribution model for a 90-psi inflation pressure and a 5400-lbf axle load is given in Table B.4.

TABLE B.1: THE 3D PRESSURE DISTRIBUTION MODEL FOR AN INFLATION PRESSURE OF 75 psi AND AN AXLE LOAD OF 4500 lbf

Along Tire Contact Length (inches) \ Along Tire Contact Width (inches)	0	0.43	1.08	1.61	2.15	3.23	4.2	5.16	6.24	6.78	7.31	8.0	8.4
0	46	59	50	33	58	63	58	62	16	67	73	52	
1.47	112	96	64	35	65	59	52	68	44	59	98	124	
2.83	134	98	98	0	45	50	46	55	15	92	98	138	
4.25	133	101	71	36	63	60	55	55	17	87	97	125	
5.67	113	100	74	34	60	49	48	74	46	56	94	111	
7.09	66	62	59	17	54	34	50	58	25	65	66	57	
8.5													

TABLE B.2: THE 3D PRESSURE DISTRIBUTION MODEL FOR AN INFLATION PRESSURE OF 90 psi AND AN AXLE LOAD OF4500 lbf

Along Tire Contact Length (inches) \ Along Tire Contact Width (inches)	0	0.43	1.08	1.61	2.15	3.23	4.2	5.16	6.24	6.78	7.31	8.0	8.4
0	23	37	46	9	37	39	48	61	7	50	55	35	
1.47	83	84	65	43	80	60	66	77	47	69	99	106	
2.83	108	97	108	27	58	54	64	69	41	83	102	126	
4.25	114	91	103	27	71	61	68	72	7	98	96	126	
5.67	87	86	68	56	75	62	68	87	57	58	99	109	
7.09	14	36	71	0	40	45	55	69	36	56	56	41	
8.5													

TABLE B.3: THE 3D PRESSURE DISTRIBUTION MODEL FOR AN INFLATION PRESSURE OF 110 psi AND AN AXLE LOAD OF 4500 lbf

Along Tire Contact Length (inches) \ Along Tire Contact Width (inches)	0	0.43	1.08	1.61	2.15	3.23	4.2	5.16	6.24	6.78	7.31	8.0	8.4
0	18	35	33	48	61	62	49	70	7	60	52	27	
1.47	68	99	94	26	82	75	72	88	52	51	99	82	
2.83	95	95	92	33	74	67	78	75	0	98	90	106	
4.25	93	103	69	57	86	74	68	82	51	58	101	99	
5.67	57	81	101	6	72	60	59	74	35	74	87	73	
7.09	2	14	42	54	58	48	55	54	27	29	34	6	
8.5													

TABLE B.4: THE 3D PRESSURE DISTRIBUTION MODEL FOR AN INFLATION PRESSURE OF 90 psi AND AN AXLE LOAD OF 5400 lbf

Along Tire Contact Length (inches)	Along Tire Contact Width (inches)											
	0	0.43	1.08	1.61	2.15	3.23	4.2	5.16	6.24	6.78	7.31	8.0	8.4
0	37	56	64	0	63	47	46	64	22	56	65	56
1.47	127	115	83	52	80	66	70	71	36	99	121	127
2.83	144	125	97	38	69	54	43	77	48	84	125	154
4.25	154	114	124	8	69	64	64	72	21	117	116	165
5.67	136	109	70	57	85	65	73	86	44	100	130	145
7.09	76	91	89	7	62	66	70	85	59	55	92	89
8.5												